



Contents lists available at [ScienceDirect](#)

## Science of the Total Environment

journal homepage: [www.elsevier.com/locate/scitotenv](http://www.elsevier.com/locate/scitotenv)



18 2



# Integrating major ion geochemistry, stable isotopes (O, H) and radioactive isotopes ( $^{222}\text{Rn}$ , $^{14}\text{C}$ , $^{36}\text{Cl}$ , $^3\text{H}$ ) to understand the interaction between catchment waters and an intermittent river

Zibo Zhou <sup>a,b,\*</sup>, Ian Cartwright <sup>a</sup>, Uwe Morgenstern <sup>c</sup>, L. Keith Fifield <sup>d</sup>

<sup>a</sup> School of Earth, Atmosphere and Environment, Monash University, Clayton, VIC 3800, Australia <sup>b</sup>

School of Engineering, Deakin University, Waurn Ponds, VIC 3216, Australia <sup>c</sup> GNS Science, Lower Hutt 5040, New Zealand

<sup>d</sup> Department of Nuclear Physics and Accelerator Applications, Research School of Physics, The Australian National University, Canberra, ACT 2601, Australia

## HIGHLIGHTS

- Intermittent rivers less well connected to regional groundwater system
- Locations and sources of baseflow investigated using geochemistry
- Mean transit times of the stream at different flow conditions estimated using radioisotopes
- Significant contribution of young near- river store in sustaining the streamflow and catchment health
- Importance of near-river environment in responding to short-term changes in climate and land use

## ARTICLE INFO

Editor: Jose Virgilio Cruz <sup>\*</sup>

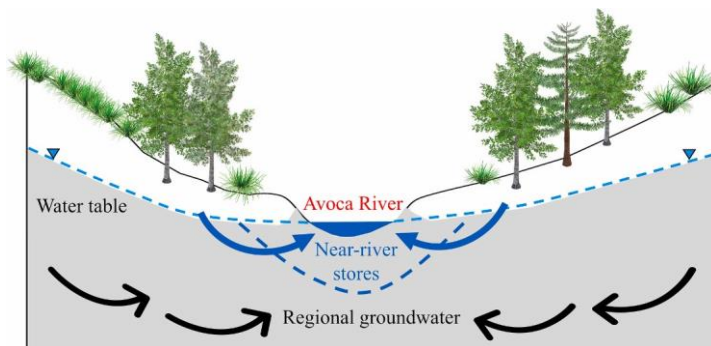
### Keywords:

Baseflow

Mean transit times Geochemistry

Intermittent streams

## GRAPHICAL ABSTRACT



## ABSTRACT

Determining the locations and sources of baseflow and the transit times of water is important for understanding catchment behaviour and functioning. Major ion geochemistry, stable isotopes ( $^{18}\text{O}$  and  $^2\text{H}$ ), and radioisotopes ( $^{222}\text{Rn}$ ,  $^3\text{H}$ ,  $^{14}\text{C}$ , and  $^{36}\text{Cl}$ ) were used to investigate the sources and transit times of water in the upper catchment of the intermittent Avoca River in southeast Australia.  $^{222}\text{Rn}$  activities and Cl concentrations implied the presence of baseflow inputs and the distribution was mainly controlled by local topography. Fluctuation of Cl concentrations implied that low-salinity near-river water was an important component of baseflow. The  $^3\text{H}$  activities of laterally disconnected pool waters during the summer months were 1.64 to 5.11 TU. The higher of these values exceed those of average annual rainfall (2.8–3.2 TU), probably due to the input of later winter to spring rainfall. The stream water had  $^3\text{H}$  activities ranging from 2.21 to 2.40 TU in July and 2.39 to 2.77 TU in August, which yield mean transit times of 4.0 to 7.0 years and 1.4 to 4.8 years respectively. These  $^3\text{H}$  activities were significantly higher than those of regional groundwater ( $^3\text{H}$  activities  $<0.1$  TU), implying that the river is largely sustained by young near-river stores at all flow conditions. Regional groundwater had  $^{14}\text{C}$  activities of 34.0 to 98.1 pMC, which yield mean residence times of up to 12,900 years.  $\text{R}^{36}\text{Cl}$  values of regional groundwater

\* Corresponding author at: School of Earth, Atmosphere and Environment, Monash University, Clayton, VIC 3800, Australia. E-mail address:

zibo.zhou@deakin.edu.au (Z. Zhou). <https://doi.org/10.1016/j.scitotenv.2023.167998>

Received 6 July 2023; Received in revised form 15 September 2023; Accepted 19 October 2023 Available online 31 October 2023

0048-9697/© 2023 The Author(s). Published by Elsevier B.V. This is an open access article under the CC BY license (<http://creativecommons.org/licenses/by/4.0/>). (50.9–61.9  $\times 10^{-15}$ ) were higher than those of modern rainfall, probably reflecting the  $\text{R}^{36}\text{Cl}$  values of recharge. Similar  $\text{R}^{36}\text{Cl}$  values of the pool and stream water (33.3–58.7  $\times 10^{-15}$ ) implied that some Cl is derived from the regional groundwater influx. As with other intermittent streams in southeast Australia, the upper Avoca River was mainly sustained by relatively small water stores, and it will be vulnerable to short-term changes in climate and land use.

## 1. Introduction

A holistic understanding of the interaction between rivers and waters stored within their catchments is essential for understanding regional hydrogeology, determining catchment water balance, predicting the hydrological response to changes in climate and land use, and effective water resources management (Sophocleous, 2002; Fleckenstein et al., 2010; Cook et al., 2018; Lewandowski et al., 2020; Barua et al., 2022; Messenger et al., 2021; Fowler et al., 2022). Baseflow represents all water stores within a catchment that sustain streamflow, especially between high flow events generated by rainfall. Baseflow comprises a number of different water sources that may change in importance during different hydrological conditions (e.g., McCallum et al., 2010; Peters et al., 2014; Rhodes et al., 2017; Cartwright and Irvine, 2020; Zhou et al., 2022). Deep regional groundwater represents the oldest and largest water store in most catchments. Younger and smaller water stores include water from the riparian zone, soil water, bank storage and return flows, and interflow (e.g., Batlle-Aguilar et al., 2014; Rhodes et al., 2017). The sources of water determine how rivers respond to short and long-term changes to climate and land use (e.g., Duvert et al., 2016; Cook et al., 2018; Richardson et al., 2020). For example, rivers connected to large reservoirs of long-lived groundwater will be more resilient to yearly variations in rainfall whereas streamflow in rivers sustained dominantly by smaller short-lived stores is likely to be more variable (Brunner et al., 2011; Fuchs et al., 2019).

$^1\text{Cl}$ , which has a half-life of 301,000 years, has traditionally been used to estimate the residence time of very old groundwater (up to 1 Ma: e.g., Phillips, 2000; Labotka et al., 2015). However, elevated  $\text{R}^{36}\text{Cl}$  values were recorded during the bomb-pulse period (Bentley et al., 1982; Phillips, 2000).  $\text{R}^{36}\text{Cl}$  values of precipitation are a function of both  $^{36}\text{Cl}$  fallout and Cl deposition. Generally,  $\text{R}^{36}\text{Cl}$  values increase with distance from the ocean due to chloride concentrations decreasing approximately exponentially with distance from the coast (Bentley et al., 1982; Keywood et al., 1998). Hence,  $\text{R}^{36}\text{Cl}$  values of precipitation at a given locality will be higher when sea levels were lower, and the climate is more continental. This may result in groundwater recharged during the Holocene when sea levels were lower having higher  $\text{R}^{36}\text{Cl}$  values than modern rainfall (Howcroft et al., 2019).

From 110 ka, sea levels around Australia declined irregularly to a maximum of  $\sim 120$  m below present day mean sea level and then rose to

### 1.1. Intermittent streams

Intermittent streams are common in semi-arid and arid regions and also locally occur in temperate and humid climates (Datry et al., 2014; Gutiérrez-Jurado et al., 2019; Shanafield et al., 2021; Barua et al., 2022; Zhou et al., 2022). They play a vital role in hosting diverse aquatic and riparian ecosystem (Stubbington et al., 2017; Shanafield et al., 2021). Especially during the periodical cease-to-flow periods, many intermittent streams contain disconnected persistent pools that support flora and fauna in riparian ecosystems (Bourke et al., 2023). Streambed infiltration from intermittent streams during dry seasons is commonly a source of recharge aquifers (e.g., Niswonger et al., 2008).

While intermittent rivers are important and account for >50 % of global rivers, our understanding of their hydrology remains incomplete compared to that of perennial streams (Datry et al., 2014; Shanafield et al., 2021; Barua et al., 2022). Perennial streams that continuously flow throughout the year are likely well connected to regional groundwater, which can sustain streamflow, especially during low flow periods (Tetzlaff and Soulsby, 2008; Cartwright et al., 2014, 2018; Duvert et al., 2016). In contrast, the connection between stream water and regional groundwater in intermittent streams may be limited, especially during the cease-to-flow periods in dry seasons when the water table may have dropped to below the streambed along many reaches (e.g., Rhodes et al., 2017; Zhou and Cartwright, 2021). Most of the water in intermittent streams may come from shallow near-river stores rather than regional groundwater. These water stores could create a buffer zone between the rivers and the regional groundwater which may limit the inflow of groundwater-borne contaminants and lessen the impacts of groundwater extraction. However, the small volume of these near-river stores potentially makes them vulnerable to short-term climate and land use changes.

### 1.2. Understanding sources of baseflow

Because the different sources of water may have different geochemistry, geochemical techniques have been successfully used to locate and quantify the inputs of baseflow into streams (McCallum et al., 2012; Zhang et al., 2013; Miller et al., 2015; Cartwright, 2022). As a result of evapotranspiration, mineral dissolution, and organic matter breakdown, the salinity of baseflow is generally higher than that of surface runoff (Herczeg et al., 2001; Edmunds, 2009) and thus, baseflow inputs are commonly marked by increases in stream salinity.  $^{222}\text{Rn}$  is an intermediate isotope in the  $^{238}\text{U}$  to  $^{206}\text{Pb}$  decay series. Because the concentration of Ra in minerals is several orders of magnitude higher than dissolved Ra concentrations in surface water,  $^{222}\text{Rn}$  activities of groundwater are higher than those in surface water (commonly 2 to 3 orders of magnitude), making  $^{222}\text{Rn}$  a useful tracer to locate and quantify baseflow inputs (Cecil and Green, 2000; Burnett and Dulaiova, 2006; Burnett et al., 2010).  $^{222}\text{Rn}$  decays with a half-life of 3.8 days and degasses to the atmosphere, hence high  $^{222}\text{Rn}$  activities indicate the presence of baseflow input (Genereux and Hemond, 1992; Cook, 2013).

Geochemistry may also be used to discern the origins of water in streams. For example, high concentrations of nitrate and organic carbon are evident in soil water due to the breakdown of organic matter (Stelzer et al., 2014). Due to seasonal recharge, evaporation, and long-term variations of stable isotope ratios of rainfall (Hughes and Crawford, 2012), different water sources may have different stable isotope ratios. Differences between downstream trends in stream water salinity and  $^{222}\text{Rn}$  activities may also be able to distinguish between the inputs of near-river stores (which is likely to have high  $^{222}\text{Rn}$  activities but low salinities) and regional groundwater (which is expected to have high  $^{222}\text{Rn}$  activities and higher salinities) (Yu et al., 2013; Ortega et al., 2015; Zhou and Cartwright, 2021).

Because the different water stores in a catchment have different residence times, radioactive isotopes such as  $^3\text{H}$  or other residence time indicators (e.g., the chlorofluorocarbons) are useful to understand the contributions of different water sources to streamflow at different locations or times. In the southern hemisphere,  $^3\text{H}$  activities of rainfall during the 1950s and 1960s (the “bomb-pulse”) were far lower than in the northern hemisphere and have now decayed to values lower than those of modern rainfall (Morgenstern et al., 2010; Tadros et al., 2014). This results in transit or residence times being more readily estimated from  $^3\text{H}$  activities and older water invariably having lower  $^3\text{H}$  activities than younger water, which is invaluable in determining relative residence times of the different water stores.

reach present day sea level between 7 and 3 ka (Chappell, 2009; Lewis et al., 2013). During the low sea level, many areas would have been further from the coast than at present and the  $\text{R}^{36}\text{Cl}$  values of rainfall would have been higher than present day values. The temporal changes in the  $\text{R}^{36}\text{Cl}$  values of precipitation account for  $\text{R}^{36}\text{Cl}$  values of groundwater in southeast Australia with  $^{14}\text{C}$  residence times of up to 20 ka being higher than those of modern precipitation (Howcroft et al., 2019). Because of the long half-life, the  $\text{R}^{36}\text{Cl}$  values of water recharged over the last few ka will be little changed and different water sources in the catchment may have a range of  $\text{R}^{36}\text{Cl}$  values. The higher  $\text{R}^{36}\text{Cl}$  values of the groundwater than regional rainfall was probably due to it being recharged during the Holocene when sea levels were lower (Howcroft et al., 2019). This makes  $^{36}\text{Cl}$  a potentially useful tracer of the water stores that sustain streamflow, however, it has rarely been employed in this way. Where groundwater has significantly higher Cl concentrations than surface water or other near-surface stores of water,  $^{36}\text{Cl}$  may also be able to detect small fluxes of groundwater that may not be apparent from other tracers.

### 1.3. Aims

This study integrates major ion geochemistry, stable isotopes ( $^{18}\text{O}$ ,  $^2\text{H}$ ), and radioactive isotopes ( $^{222}\text{Rn}$ ,  $^{14}\text{C}$ ,  $^3\text{H}$ , and  $^{36}\text{Cl}$ ) to understand the different water sources in the intermittent upper Avoca River in southeast Australia. In particular, it represents one of only a few studies globally to determine the residence times of water sustaining an intermittent river. It also explores the use of  $^{36}\text{Cl}$  in distinguishing the sources of solutes and water in rivers, which will have applications in other catchments. The results of this study will improve our general understanding of the functioning of intermittent streams, in particular by determining the connection with regional groundwater and the vulnerability to climate variability, which are important but currently poorly known.

## 2. Study area

The Avoca River that is located in northwest Victoria is an intermittent river in the Murray-Darling Basin. The area of the whole catchment is approximately 14,000 km<sup>2</sup> (Department of Environment, Land, Water and Planning, 2022). The river originates in the Great Dividing Ranges near Amphitheatre (Fig. 1), flows north for 280 km and terminates in Lake Bael Bael and the Avoca Marshes near the Murray River (Lorimer and Rowan, 1982; Smith, 1995). The elevation of the catchment is up to 784 m at headwaters in mountain ranges and decreases to 141 m in the north (Bureau of Meteorology, 2022). The river occupies a confined valley from its headwaters to Charlton (Fig. 1) with a wider floodplain downstream that has many wetland areas. The study area is located in the upper catchment of the Avoca River between the headwaters and Charlton (Fig. 1). Dryland pasture with larger stands of native woodlands along the floodplain are main type of vegetations in the upper catchment and native plantation forests are dominant in the headwaters (North Central Catchment Management Authority, 2007; Department of Environment, Land, Water and Planning, 2022). The geology of the upper Avoca catchment includes a basement of Palaeozoic metamorphosed turbidites (the Castlemaine Group and St Arnaud Group) and Devonian Granites. These are overlain by small basaltic lava plains of the Newer Volcanic Group and fluvial sediments that have rounded gravels, coarse sands, silts and clays (Lorimer and Rowan, 1982).

The average annual rainfall in the upper Avoca catchment decreases northwards from 536 mm at Amphitheatre to 420 mm at Charlton (Bureau of Meteorology, 2022). Winter (June to August) is the wettest season while the summer months have the lowest rainfall (Bureau of Meteorology, 2022). Streamflow is higher in the winter and spring and a series of persistent pools are formed during the time when the river ceases to flow in the summer. The average annual streamflow between 2000 and 2020 ranged from  $1.1 \times 10^5$  to  $1.2 \times 10^8$  m<sup>3</sup>/year at Amphitheatre and  $1.3 \times 10^5$  to  $2.3 \times 10^8$  m<sup>3</sup>/year at Coonooer (Department of Environment, Land, Water and Planning, 2022).

Most tributaries along the river are ephemeral and dry except immediately after major rainfall. Amphitheatre and Fentons Creeks are the largest of the tributaries in the upper Avoca catchment (Fig. 1). These flow for longer periods of the year, although their discharge is much lower than the main river (Department of Environment, Land, Water and Planning, 2022). Groundwater is recharged on the higher ground at the catchment margins and flows from south to north (North Central Catchment Management Authority, 2007). The total dissolved solids (TDS) of the groundwater varies from <560 mg/L in some of the basalts to up to 3360 mg/L in some of the aquifers (Heislars, 1993; Department of Environment, Land, Water and Planning, 2022). Surface water and groundwater in the upper Avoca catchment are locally used for domestic and irrigation purposes (North Central Catchment Management Authority, 2007).

### 3. Materials and methods

#### 3.1. Sampling

Twenty-six samples of pool water were collected from laterally disconnected pools (Fig. 1) on 26–28 of March in 2019 when the upper Avoca River had ceased to flow during the summer months (Fig. 2). Two rounds of stream water sampling (28 samples each round) were conducted on 8–10 of July and 24–26 of August in 2019 when the upper Avoca River was flowing (Fig. 1, Table S1). Samples were also collected from Amphitheatre Creek and Fentons Creek (Fig. 1) at their confluences with the main river; in March 2019 these tributaries also consisted of laterally-disconnected pools. An open sample collector was used for river water sampling from the centre of the river. Continuous streamflow and electrical conductivity are measured at Amphitheatre and Coonooer (Figs. 1, 2; Department of Environment, Land, Water and Planning, 2022). Continuous streamflow is also measured at Archdale Junction and river depth (but not streamflow) is measured at Charlton (Fig. 1; Department of Environment, Land, Water and Planning, 2022). Groundwater was sampled in May 2019 from groundwater monitoring bores (Fig. 1). Several volumes of water were purged from the bore prior to sampling using an impellor pump or the bores were pumped dry and sampled following recovery.

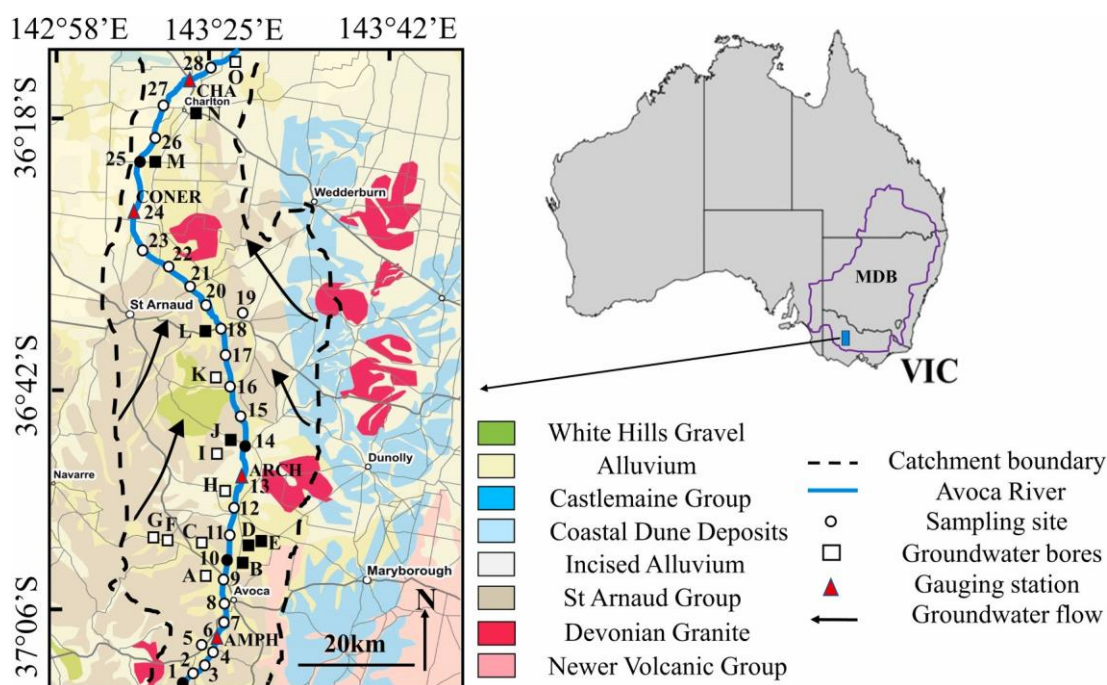


**Fig. 1.** Geological and hydrogeological map of the upper Avoca River. Stream sampling sites and groundwater bores are indicated by numbers and letters, respectively. The inset shows the location in Victoria (VIC) and the Murray-Darling Basin (MDB). The sites that have <sup>14</sup>C, <sup>3</sup>H, and/or <sup>36</sup>Cl data are shown in solid symbols. Gauging stations with site number are Amphitheatre (AMPH; 408202), Archdale Junction (ARCH; 408206), Coonooer (CONER; 408200), and Charlton (CHA; 408212). Background geological map from Department of Jobs, Precincts and Regions (2022).

### 3.2. Analytical techniques

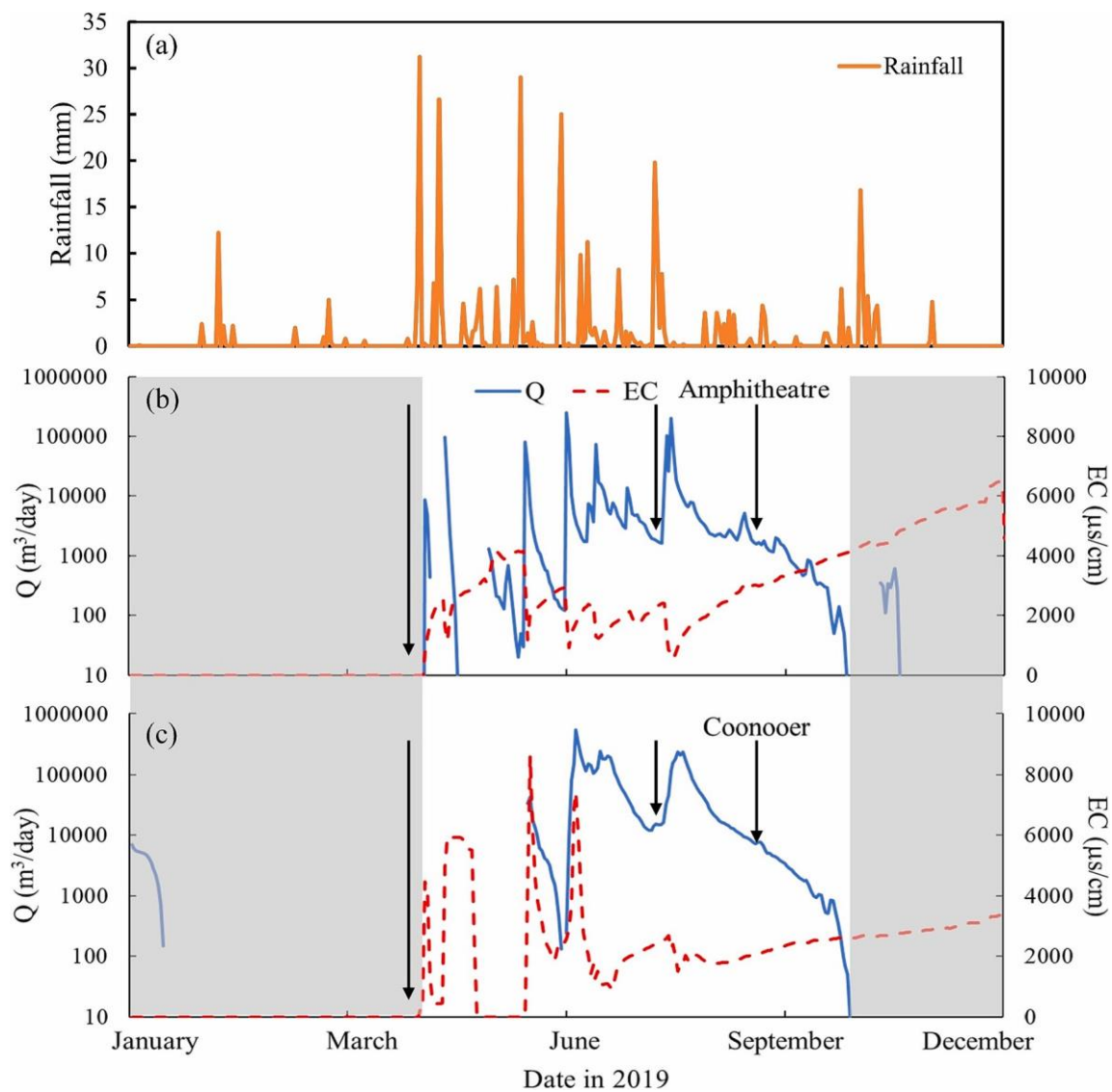


**Fig. 2.** Variations in rainfall (2a) in the upper Avoca Catchment and EC and Q (streamflow) at Amphitheatre (2b) and Coonooer (2c) ([Fig. 1](#)) in the upper Avoca River in 2019 (missing data during the flow period are caused by equipment failure). Shaded areas indicate the cease-to-flow period. Sampling times are indicated by arrowed lines. Data from [Department of Environment, Land, Water and Planning \(2022\)](#) and [Bureau of Meteorology \(2022\)](#).

Electrical Conductivity (EC) was measured in the field using a calibrated TPS meter and electrode. Cation and anion concentrations were



determined at Monash University using a Thermo Fischer ICP-OES and a Thermo Fischer ion chromatograph, respectively. Samples were filtered through 0.45 µm cellulose nitrate filters and acidified to pH < 2 for cation measurements and filtered and unacidified for anion measurements. Overall precision ( $\sigma$ ) of major ion concentrations is 2–5 % based on replicate analyses. Stable isotope analyses were performed at Monash University using a Thermo Finnigan Delta Plus Advantage mass spectrometer.  $\delta^{18}\text{O}$  values were analysed via equilibration with  $\text{He-CO}_2$  at 32 °C for 24–48 h in a Thermo Finnigan Gas Bench.  $\delta^2\text{H}$  values were determined following reduction of  $\text{H}_2\text{O}$  by Cr at 850 °C in a Finnigan MAT H/Device. Values of  $\delta^{18}\text{O}$  and  $\delta^2\text{H}$  were normalised as described by Coplen (1988) and are expressed relative to V-SMOW. Precision ( $\sigma$ ) based on replicate analyses is 0.15 ‰ for  $\delta^{18}\text{O}$  and 1 ‰ for  $\delta^2\text{H}$ .

$^{222}\text{Rn}$  activities were measured in the field using portable radon-in-air detectors (DurrIDGE Corporation RAD-7).  $^{222}\text{Rn}$  was degassed from 500 ml of water for 5 min into a closed air loop of known volume and counting times were 2 h for surface water and 30 mins for groundwater.  $^{222}\text{Rn}$  activities are reported as Bq/m<sup>3</sup> (becquerels per m<sup>3</sup>) with a precision of ~3 % at 10,000 Bq/m<sup>3</sup> and ~10 % at 100 Bq/m<sup>3</sup>.

After vacuum distillation and electrolytic enrichment,  $^3\text{H}$  activities were measured at the Institute of Geological and Nuclear Sciences (GNS) in New Zealand using liquid scintillation in Quantulus ultra-low-level counters (Morgenstern and Taylor, 2009).  $^3\text{H}$  activities are reported in Tritium Units (TU) where 1 TU corresponds to  $^3\text{H} / \text{H} = 10\text{--}18$  with a 0.02 TU detection limit and relative uncertainties ( $1\sigma$ ) ~  $\pm 2$  %.  $^{14}\text{C}$  activities of groundwater were determined by using accelerator mass spectrometry (AMS) at GNS in New Zealand (Stewart et al., 2004). Orthophosphoric acid was utilised to collect  $\text{CO}_2$  from the groundwater, and after being purified under vacuum, the captured  $\text{CO}_2$  was changed into a graphite target. Percent modern carbon (pMC) is used to report  $^{14}\text{C}$  activities and the modern  $^{14}\text{C}$  activity is considered to be 95 % of the  $^{14}\text{C}$  activity of the NBS oxalic acid standard in 1950.  $^{36}\text{Cl}$  analyses were conducted by using the 14UD accelerator at the Australian National University as described by Fifield et al. (2013).  $^{36}\text{Cl}$  activities are reported as  $R^{36}\text{Cl}$  ( $^{36}\text{Cl}/\text{Cl} \times 10^{-15}$ ).  $R^{36}\text{Cl}$  uncertainties ranged from 5 to 6 %. The complete geochemistry dataset is in the Supplement (Tables S1 and S2).

### 3.3. Mean residence and mean transit times

Mean transit times (MTTs), which represent the time taken for water to flow through the catchment from where it was recharged to where it discharges into the stream, were calculated using lumped parameter model (LPMs) from the river  $^3\text{H}$  activities. The convolution integral:

$$C_0(t) = \int_0^\infty C_i(t-\tau)g(\tau)e^{-\lambda\tau}d\tau \quad (1)$$
 relates the input of  $^3\text{H}$  ( $C_i$ ) in rainfall overtime to the  $^3\text{H}$  activity of stream water sampled at time  $t$  ( $C_0(t)$ ). In eq. (1),  $t-\tau$  is the time that the water was recharged,  $\tau$  is the transit time,  $\lambda$  is the decay constant of  $^3\text{H}$  ( $0.0563 \text{ yr}^{-1}$ ), and the function  $g(\tau)$  describes the distribution of flow paths and transit times in the system. Annual weighted  $^3\text{H}$  activities of rainfall in Melbourne (Tadros et al., 2014) were used as the  $^3\text{H}$  input. Predicted present-day  $^3\text{H}$  activities of annual rainfall in central Victoria are 2.8 to 3.2 TU (Tadros et al., 2014) and the measured  $^3\text{H}$  activities in that region are within that range (Cartwright and Morgenstern, 2015; Cartwright et al., 2018; Howcroft et al., 2018; Barua et al., 2022). The LPMs used are implemented in the TracerLPM Excel workbook (Jurgens et al., 2012). Given that the geometry of the flow systems in the Avoca catchment are not explicitly known and may be spatially variable, a range of LPMs were used. The Exponential Mixing Model (EMM) represents flow systems in which transit times are exponentially distributed. The Exponential Piston Flow Model (EPM) describes aquifers with both exponential and piston-flow sections. The EPM is commonly employed in unconfined aquifers that have exponential flow below the water table and vertical recharge in the unsaturated zone (Maloszewski, 2000; Morgenstern et al., 2010; Howcroft et al., 2019). The EPM ratio describes the relative ratio of piston and exponential flow; here EPM ratios of 0.33 (75 % exponential flow) and 1 (50 % exponential flow) were used. The dispersion model (DM), which is based on the one-dimensional advection-dispersion-transport equation, can be used in a number of aquifer configurations (Zuber and Maloszewski, 2001; McGuire and McDonnell, 2006; Jurgens et al., 2012). This model includes the dispersion parameter ( $D_r$ ) which is the ratio of dispersion to advection and is the inverse of the Peclet Number.  $D_r$  values of 0.05 to 0.5 are suggested for kilometre-scale flow systems (Maloszewski, 2000; Zuber and Maloszewski, 2001) and were used here. The estimates of MTTs are based on single samples. While the much lower bomb-pulse  $^3\text{H}$  activities preclude testing of the LPMs using time-series measurements that commenced over recent years (Cartwright and Morgenstern, 2015), this approach has reproduced stream water time-series  $^3\text{H}$  activities elsewhere (Maloszewski and Zuber, 1982; Blavoux et al., 2013; Morgenstern et al., 2015).

The lumped parameter models were also used to estimate mean residence time (MRTs) in groundwater and calculate  $^{14}\text{C}$  vs.  $^3\text{H}$  trends. Here the EPM, which may be used where wells are not fully penetrating and sample only part of the flow system (Maloszewski and Zuber, 1982; Morgenstern et al., 2015), is used. The  $^{14}\text{C}$  activities of atmospheric  $\text{CO}_2$  in the southern hemisphere were used as the input function (McCormac et al., 2004; Reimer et al., 2013). As elsewhere in southeast Australia, (Cartwright et al., 2013; Meredith et al., 2016), the aquifers in the Avoca Catchment contain calcite cements and veins, which likely have variable  $\delta^{13}\text{C}$  values and isotope mass balance is not viable to estimate closed-system calcite dissolution. However, the aquifers are siliceous and closed-system calcite dissolution is probably <10 % (Clark, 2015). In these calculations, values of  $q$  (the fraction of DIC derived from the recharging water) between 1 (all DIC derived from recharge) and 0.9 (10 % contribution of  $^{14}\text{C}$ -free DIC from the aquifer matrix) were used.

## 4. Results

### 4.1. Streamflow

The variations of streamflow and EC at the Amphitheatre and Coonooer (Fig. 1) in 2019 are shown in Fig. 2. Streamflow at Archdale Junction and water levels at Charlton (Fig. 1) show similar patterns. A short period of relatively high streamflow (up to 6980 m<sup>3</sup>/day) was recorded at Coonooer in early 2019 following rainfall in late 2018. However, the upper Avoca River largely comprised disconnected water pools during the summer months from January to April. The river started to flow from early May 2019 and streamflow reached a peak in June (up to  $2.5 \times 10^5$  m<sup>3</sup>/day at Amphitheatre and  $5.6 \times 10^5$  m<sup>3</sup>/day at Coonooer). Streamflow then gradually decreased from August and the river ceased to flow in later October. During the sampling periods in July and August, the daily streamflows were 5900 m<sup>3</sup>/day and 2806 m<sup>3</sup>/day at Amphitheatre and  $1.3 \times 10^5$  m<sup>3</sup>/day and  $3.6 \times 10^4$  m<sup>3</sup>/day at Coonooer (Fig. 2).



#### 4.2. Major ion geochemistry and $^{222}\text{Rn}$

EC values of stream water in 2019 in the headwaters at Amphitheatre were generally lower (1000–4000  $\mu\text{S}/\text{cm}$ ) than further downstream at Coonooer (up to 8629  $\mu\text{S}/\text{cm}$ ) (Fig. 2). EC values at both gauges were variable but were generally lower during the high winter flows (Fig. 2). Short-term increases in EC occasionally observed at the onset of higher flows probably represent the mobilisation of saline water stored in the soils, regolith, or near-river aquifers. Na and Cl are the most abundant cation (78–86 % on a molar basis) and anion (85–98 % on a molar basis), respectively, in the stream water (Table S1). During July and August when the upper Avoca River was flowing, Cl concentrations were between 230 and 1640 mg/L (Fig. 3b). Unlike many rivers where Cl concentrations increase downstream due to groundwater inflows (Yu et al., 2013; Ortega et al., 2015), there is no consistent trend in Cl concentrations.  $^{222}\text{Rn}$  activities (Fig. 3a) were up to 2920 Bq/m<sup>3</sup> in the headwaters and generally decreased downstream to <1000 Bq/m<sup>3</sup>. Locally higher  $^{222}\text{Rn}$  activities were recorded between 8 and 36 km (Fig. 3a).

The water from the disconnected pools in the summer months is much more saline than when the river was flowing, with EC values of 2220–14,070  $\mu\text{S}/\text{cm}$  (Table S1). Cl concentrations during the cease-to-flow period were 726 to 12,772 mg/L and were higher in the middle and lower reaches of the river (Fig. 3). The concentrations of the other major ions have similar spatial and temporal trend to Cl (Table S1).  $^{222}\text{Rn}$  activities of the pool have a similar trend to when the river

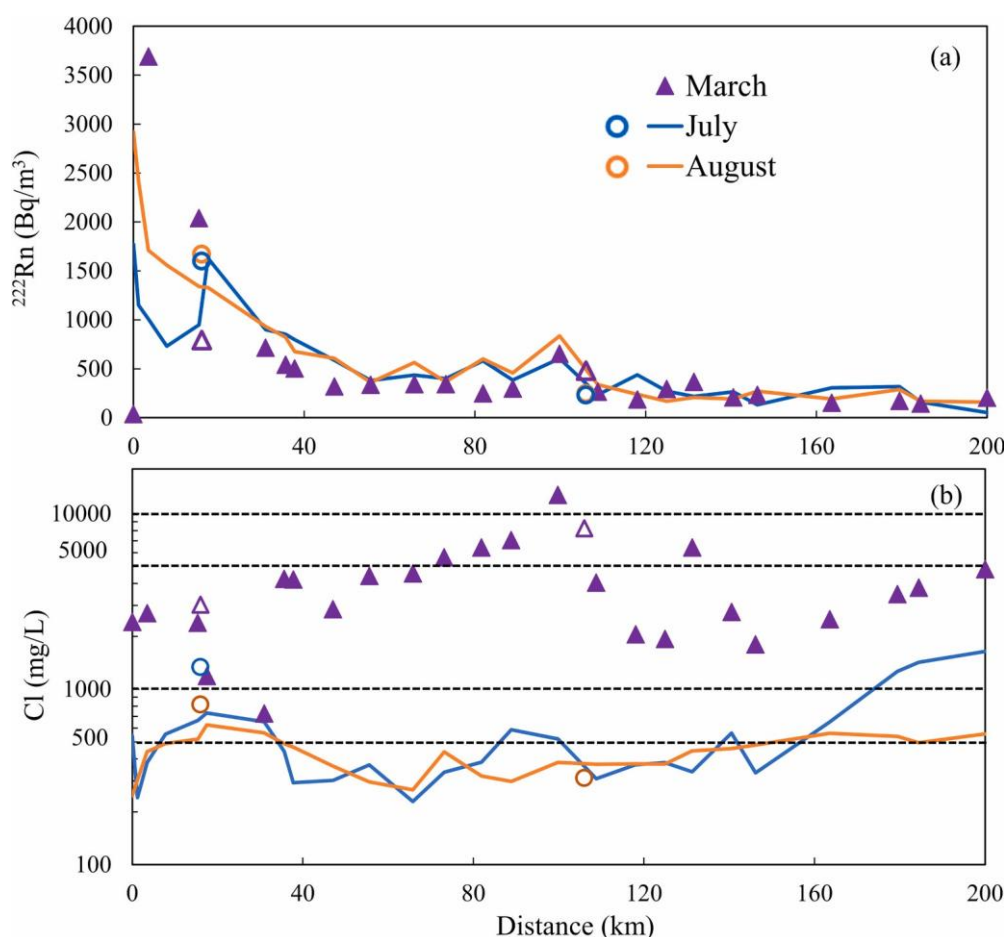


**Fig. 3.** Downstream variations in  $^{222}\text{Rn}$  (3a) and Cl concentrations (3b) during different flow conditions in the upper Avoca River. Solid symbols represent pool water samples and open symbols are tributaries. Dash lines are used to indicate Cl concentrations. Data from Tables S1 and S2.

was flowing. The major ion geochemistry and  $^{222}\text{Rn}$  activities of the major tributaries (Amphitheatre Creek and Fentons Creek) are similar to the main river near their confluences (Table S1, Fig. 3). Molar Cl/Br ratios in the stream water and pool water are  $(846 \pm 209$  and  $955 \pm 623$ , respectively (Table S1). While these are variable, they are far below those that would result from halite dissolution (typically 10,000–15,000; Davis et al., 1998).

Regional groundwater had EC values of 1643–12,060  $\mu\text{S}/\text{cm}$  (mean =  $5763 \pm 1581$   $\mu\text{S}/\text{cm}$ ). Na concentrations were 362 to 4578 mg/L (mean =  $1883 \pm 589$  mg/L) and Cl concentrations were between 489 and 6832 mg/L (mean =  $2998 \pm 953$  mg/L). The concentrations of these and other major ions were correlated with EC (Table S2).  $^{222}\text{Rn}$  activities in the regional groundwater ranged from 2470 to 107,000 Bq/m<sup>3</sup> with a mean value of  $29,912 \pm 29,620$  Bq/m<sup>3</sup>. There is no difference in the major ion geochemistry of groundwater from the different formations (Table 2, Fig. 1) or any systematic difference with position in the catchment. The major ion ratios of the pool water and river water overlap. However, the groundwater has slightly higher relative Na and K concentrations (Fig. 4). Molar Cl/Br ratios in the groundwater ( $722 \pm 85$ , Table S2) again suggest that there has been no significant halite dissolution. The observation that concentrations of Ca (relative to the other cations) and  $\text{HCO}_3^-$  (relative to the other anions) are low (Fig. 4) is consistent with their being limited calcite dissolution.

#### 4.3. Stable isotopes

Water from the laterally-disconnected pools had a wide range of  $\delta^2\text{H}$  and  $\delta^{18}\text{O}$  values that varied from  $-23$  ‰ to  $+44$  ‰ and  $-4.1$  ‰ to  $+12.3$  ‰, respectively (Tables S1 and S2, Fig. 5). These values define an array with a slope of 4.1 to the right of Melbourne meteoric water line that reflects evaporation during the summer months. (Gonfiantini, 1986; Clark and Fritz, 1997). This array intercepted the Melbourne meteoric water line close to the weighted average  $\delta^{18}\text{O}$  and  $\delta^2\text{H}$

values of Melbourne rainfall ( $\delta^{18}\text{O} = -4.98\text{‰}$ ,  $\delta^2\text{H} = -28.4\text{‰}$ ; Hollins et al., 2018). The upper Avoca River in July and August had  $\delta^{18}\text{O}$  and  $\delta^2\text{H}$  values that plot on the Melbourne meteoric water line and cluster around those of average Melbourne rainfall.  $\delta^{18}\text{O}$  and  $\delta^2\text{H}$  values in July ranged from

$-3.3$  to  $-6.1\text{‰}$  (mean =  $-4.7 \pm 0.2\text{‰}$ ) and  $-17$  to  $-33\text{‰}$  (mean =

$-23 \pm 1.9\text{‰}$ ), respectively, whereas in August, the values were  $-2.6$  to  $-5.3\text{‰}$  (mean =  $-4.6 \pm 0.2\text{‰}$ ) and  $-11$  to  $-30\text{‰}$  (mean =  $-26 \pm 1.5\text{‰}$ ), respectively (Table S1). The  $\delta^{18}\text{O}$  and  $\delta^2\text{H}$  values of groundwater were slightly lower ( $-4.1$  to  $-7.7\text{‰}$ , mean =  $-5.5 \pm 0.4\text{‰}$  and  $-27$  to  $-52\text{‰}$ , mean =  $-34 \pm 2.2\text{‰}$ ) than those of the river water and the pool

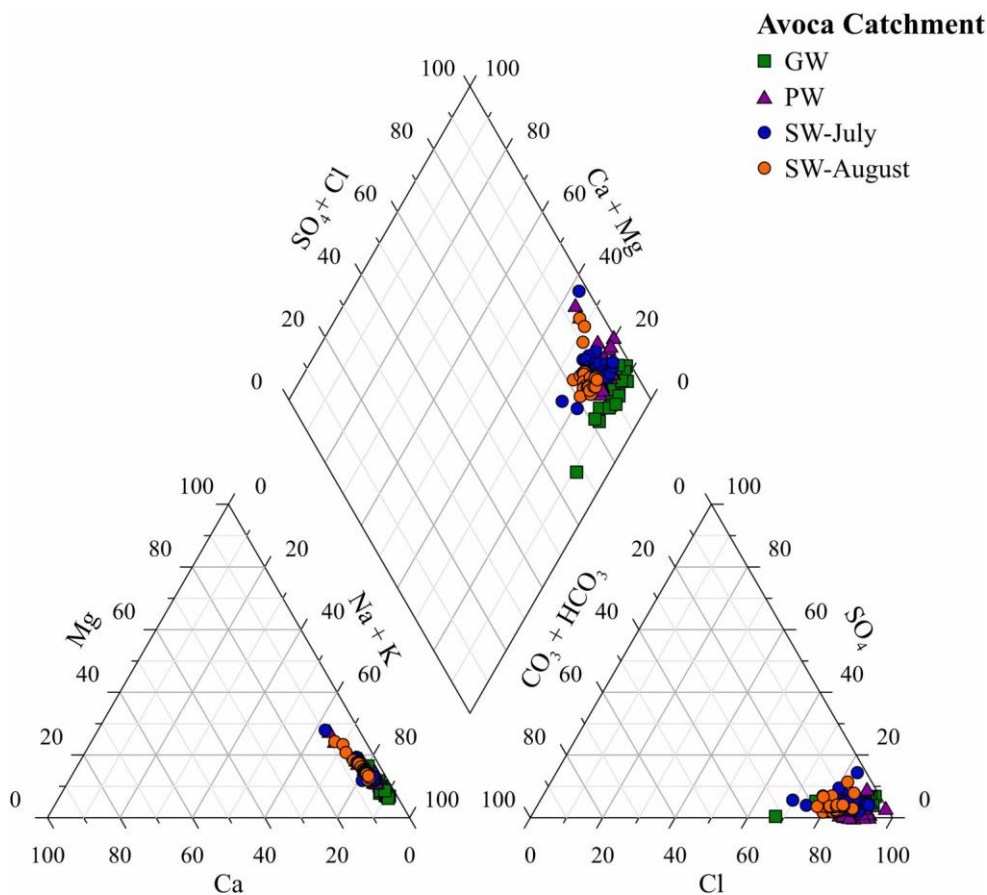
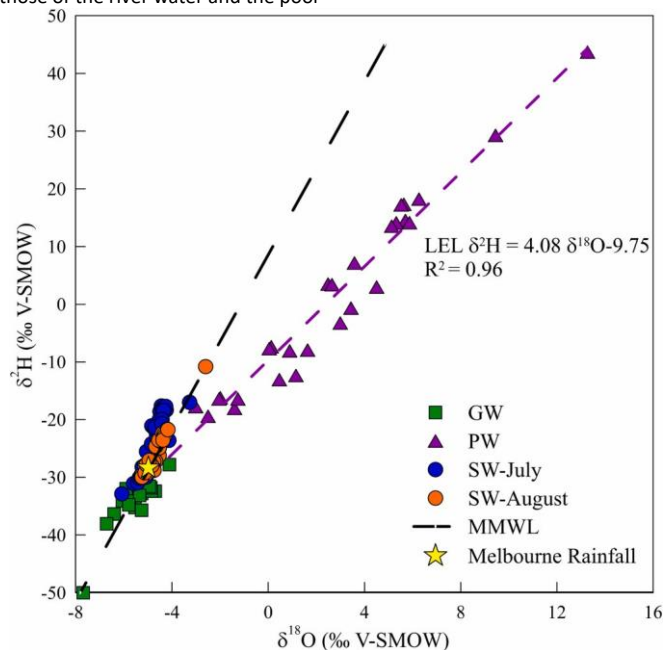


Fig. 4. Piper diagram of the different water sources in the Avoca Catchment (data from Tables S1 and S2). GW = groundwater; PW = pool water; SW = stream water.

**Fig. 5.** Stable isotope ratios of water samples in the Avoca catchment. MMWL = Melbourne Meteoric Water Line ( $\delta^2\text{H} = 7.4 \times \delta^{18}\text{O} + 8.6$  ‰, as defined by Hughes and Crawford, 2012). GW = regional groundwater; PW = pool water; SW = stream water. The LEL (local evaporation line) is the best fit for the pool water data. Data from Tables S1 and S2. waters (Fig. 5; Table S2).

#### 4.4. Radioactive isotopes ( $^3\text{H}$ , $^{14}\text{C}$ , and $^{36}\text{Cl}$ )

##### 4.4.1. Regional groundwater

$^3\text{H}$  activities in regional groundwater ranged from below detection ( $< 0.02$ ) to 1.08 TU (Table 1). These are much lower than the predicted and measured weighted average activities of modern rainfall in this area ( $3.0 \pm 0.2$  TU: Tadros et al., 2014; Cartwright and Morgenstern, 2015; Cartwright et al., 2018; Howcroft et al., 2018; Barua et al., 2022). There is no decreasing trend of  $^3\text{H}$  activities with depth in the groundwater. Groundwater from sites J and M (Fig. 1) that have  $^3\text{H}$  activities  $> 0.1$  TU

**Table 1**

$^3\text{H}$ ,  $^{14}\text{C}$  activities, and MTTs calculated using the exponential piston-flow model (EPM; ratio = 0.33) of groundwater from the upper Avoca River Catchment. Letters in brackets represent locations site on Fig. 1.

Bore ID	Depth m	$\text{R}^{36}\text{Cl}$ 10 <sup>-15</sup>	$^3\text{H}$ TU	$^{14}\text{C}$ pMC	MTTs- $^3\text{H}$ Years	MTTs- $^{14}\text{C}$ Years
8003924 (B)	42	60.6	0.06	34.0	nc1 nc	12,900
8003936 (D)	12	50.9	bd <sub>2</sub>	93.9		500
8003934 (E)	58	51.1	bd	70.2	nc	3201
8003932 (J)	17	61.9 59.1	0.04	73.6	nc mixed <sup>3</sup>	2700
8003933 (J)	60		1.08	61.6		mixed
109570 (L)	30	53.6	bd	58.4	nc	5401
110184 (M)	30	58.5	0.16	93.5	201	nc
110185 (M)	13	56.5	0.29	98.1	151	nc
119378 (N)	11	54.7	0.06	88.9	nc	1000

1 nc = not calculated.

2 bd = below detection.

3 sample showing mixing between old and young water (Fig. 6).

are within 200 m of the river (Fig. 1 and Table 2).  $^{14}\text{C}$  activities of regional groundwater were 34.0–98.1 pMC (Table 1). Groundwater with the highest  $^{14}\text{C}$  activities (98.1 pMC) also had measurable  $^3\text{H}$  activities (0.29 TU). Groundwater that does not undergo mixing of old and young water within aquifers following recharge has predictable  $^{14}\text{C}$  and  $^3\text{H}$  activities governed by the relative decay rates of those two isotopes (Fig. 6b) (Le Gal La Salle et al., 2001; Cartwright et al., 2019). Mixing of young (high  $^{14}\text{C}$  and  $^3\text{H}$ ) and old (low  $^{14}\text{C}$  and  $^3\text{H}$ -free) water in aquifers produces groundwater with low to moderate  $^{14}\text{C}$  activities but measurable  $^3\text{H}$  activities (Fig. 6b). The majority of groundwater samples from the upper Avoca River have  $^{14}\text{C}$  and  $^3\text{H}$  activities that imply that significant mixing has not occurred. Only 60 m deep groundwater from adjacent to the Avoca River at Archdale Reserve (bore 8003933 from site J: Fig. 1) shows evidence of mixing (Fig. 6b).

$\text{R}^{36}\text{Cl}$  values of the groundwater had a range of 50.9–61.9  $\times 10^{-15}$  (Fig. 6 and Table 1), which is higher than those of local modern rainfall in northern Victoria ( $15\text{--}35 \times 10^{-15}$ : Davie et al., 1989; Cartwright et al., 2017; Howcroft et al., 2019). This is similar to the Barwon catchment in southeast Australia that  $\text{R}^{36}\text{Cl}$  values of groundwater were up to  $53.7 \times 10^{-15}$  and the local rainfall was in a range of 14 to  $20 \times 10^{-15}$  (Howcroft et al., 2019).  $\text{R}^{36}\text{Cl}$  values do not correlate with  $^{14}\text{C}$  and  $^3\text{H}$  activities (Fig. 6) or Cl concentrations (Fig. 7a).

##### 4.4.2. Stream water

During the cease-to-flow period in the summer,  $^3\text{H}$  activities ranged from 1.64 to 5.11 TU (Fig. 6a; Table 2), which are higher than all of the groundwater  $^3\text{H}$  activities. The pool waters with  $^3\text{H}$  activities higher than the average of local modern rainfall ( $3.0 \pm 0.2$  TU) were downstream of Logan Reserve (109 km). The  $^3\text{H}$  activities when the river was flowing were 2.21 to 2.67 TU in July and 2.39 to 2.77 TU in August, which were lower than those of average rainfall and again higher than

**Table 2**

those of the groundwater (Table 1).

$\text{R}^{36}\text{Cl}$  values of the upper Avoca River were lowest in the headwaters ( $< 40 \times 10^{-15}$ ) and increased downstream to  $40\text{--}60 \times 10^{-15}$  (Fig. 7b; Table 2). No significant difference is detected between the  $\text{R}^{36}\text{Cl}$  values of the pool water and the river water from July and August, and the highest  $\text{R}^{36}\text{Cl}$  values overlapped with those of the groundwater (Fig. 6a). Aside from the pool water with  $^3\text{H}$  activities higher than modern rainfall, the  $^3\text{H}$  activities and  $\text{R}^{36}\text{Cl}$  values in the Avoca River lie close to the mixing trend between rainfall and regional groundwater.

## 5. Discussion

The stable and radioactive isotopes together with major ion geochemistry help determine baseflow locations, water sources, and MTTs/MRTs in the upper Avoca River and the groundwater. The data indicate that the upper Avoca River receives water from several stores, but that regional groundwater is not the most important contributor to baseflow and that several near-river stores are important. This has implications for quantifying baseflow inputs and understanding the vulnerability of the stream and its ecosystems.

### 5.1. Sources of water contributing to the Avoca River

In common with rivers elsewhere (e.g., the Maribyrnong catchment, in southeast Australia: [Cartwright and Gilfedder, 2015](#); the Coyote Creek, in northern California, USA: [Bogan et al., 2019](#)) that contain permanent pools in dry seasons, the persistence of the pools suggests that the upper Avoca River receives water from several catchment stores over the summer months. The  $^{222}\text{Rn}$  activities of the pool water were 38–9480 Bq/m<sup>3</sup> with a median value of 309 Bq/m<sup>3</sup> ([Fig. 3a](#)), which are generally higher than if the pools were only fed by surface water (e.g.,

$^3\text{H}$  activities,  $\text{R}^{36}\text{Cl}$  values and MTTs from pool water and stream water of the upper Avoca River.

Sample ID <sup>1</sup>	Distance <sup>2</sup> km	$^3\text{H}$ TU	$\text{R}^{36}\text{Cl}$ 10–15	MTTs (years) <sup>3</sup> DM <sup>4</sup> (0.05)	DM (0.5)	EPM <sup>5</sup> (0.33)	EPM (1.0)	EMM <sub>3</sub>
March 2019 <sup>4</sup> Headwaters								
(1)	0	2.36	31.9	nc <sup>5</sup>	nc	nc	nc	nc
Amphitheatre (6)	15	1.64	45.6	nc	nc	nc	nc	nc
Bealiba (10)	38	2.79	42.1	nc	nc	nc	nc	nc
Arch Res (14)	73	1.89	57.7	nc	nc	nc	nc	nc
Logan Res (18)	109	4.57	66.9	nc	nc	nc	nc	nc
Coonoor (24)	146	5.11	60.8	nc	nc	nc	nc	nc
Seven Mile (25)	164	5.03	57.2	nc	nc	nc	nc	nc
Boort (28)	191	4.42	56.6	nc	nc	nc	nc	nc
July 2019								
Headwaters (1)	0	2.40	33.3	4.0	4.6	4.2	4.0	4.6
Amphitheatre (6)	15	2.21	58.5	5.5	6.8	6.2	5.7	7.0
Archdale Res (14) Logan	73	2.23 nm <sup>6</sup>	55.1 42.1	5.4 nc	6.6 nc	6.0 nc	5.6 nc	6.7 nc
Res (18)	109							
Coonoor (24)	146	nm	59.2	nc	nc	nc	nc	nc
Seven Mile (25)	164	2.22	58.7	5.6	6.7	6.1	5.7	6.8
August 2019								
Headwaters (1)	0	2.67	36.4	2.1	2.2	2.1	2.1	2.2
Amphitheatre (6)	15	2.39	42.6	4.1	4.7	4.4	4.2	4.8
Archdale Res (14)	73	2.77	54.3	1.4	1.5	1.4	1.4	1.5
Logan Res (18)	109	nm	54.1	nc	nc	nc	nc	nc
Coonoor (24)	146	nm	47.9	nc	nc	nc	nc	nc
Seven Mile (25)	164	2.57	50.3	2.8	3.0	2.9	2.8	3.0

1 Numbers in brackets represent location site on [Fig. 1](#).

2 Distance downstream from headwater site.

3 MTTs calculated using the dispersion model (DM:  $D_p$  in brackets), exponential piston-flow model (EMP: EPM ratio in brackets), and exponential mixing model (EMM).

4 Cease-to-flow period.

5 nc = not calculated.

6 nm = not measured.

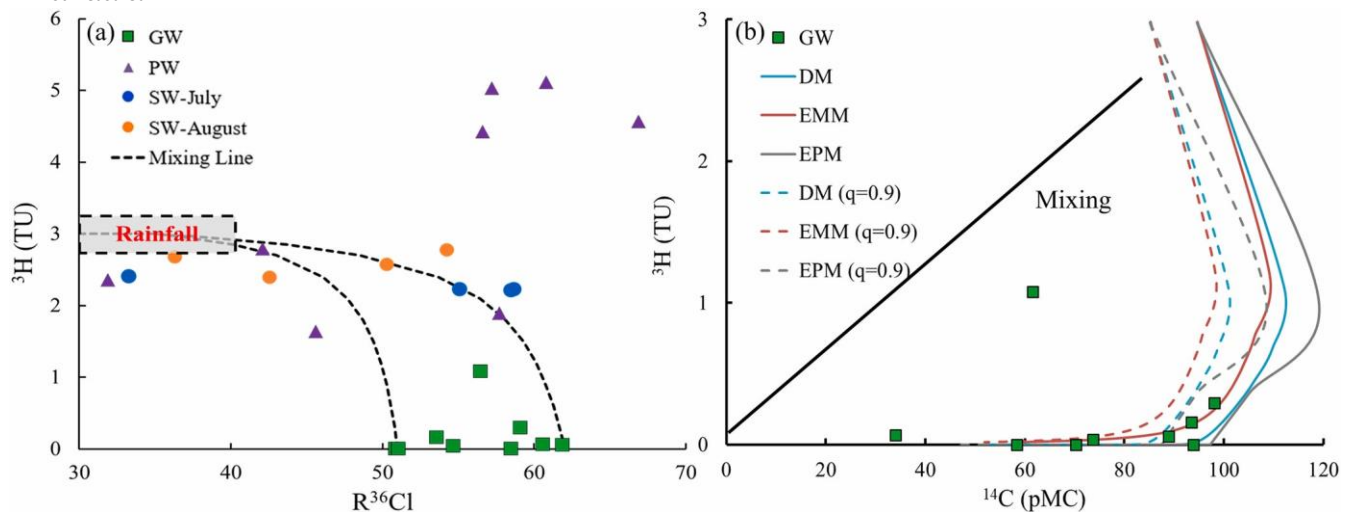


**Fig. 6.**  $^3\text{H}$  activities vs.  $\text{R}^{36}\text{Cl}$  (6a) of groundwater (GW), pool water (PW), and stream water (SW) from the upper Avoca River. The shade area represents the modern rainfall in the region ([Tadros et al., 2014](#); [Howcroft et al., 2019](#)) and the curved lines show schematically the effects of mixing between rainfall and groundwater.  $^3\text{H}$  activities vs.  $^{14}\text{C}$  activities (6b) of groundwater from the upper Avoca River. Curved lines are the covariance in the radioisotopes predicted by the Exponential Mixing, Exponential-Piston (EPM ratio = 1), and Dispersion ( $D_p = 0.5$ ) lumped parameter models. Calcite dissolution lowers the predicted  $^{14}\text{C}$  activities (dashed lines display trends with 10 % calcite dissolution). Solid line shows schematically the effects of mixing between old regional groundwater (low  $^{14}\text{C}$  and  $^3\text{H}$  free) and modern or recently recharged water (high  $^{14}\text{C}$  and  $^3\text{H}$ ). Data from [Tables 1 and 2](#).

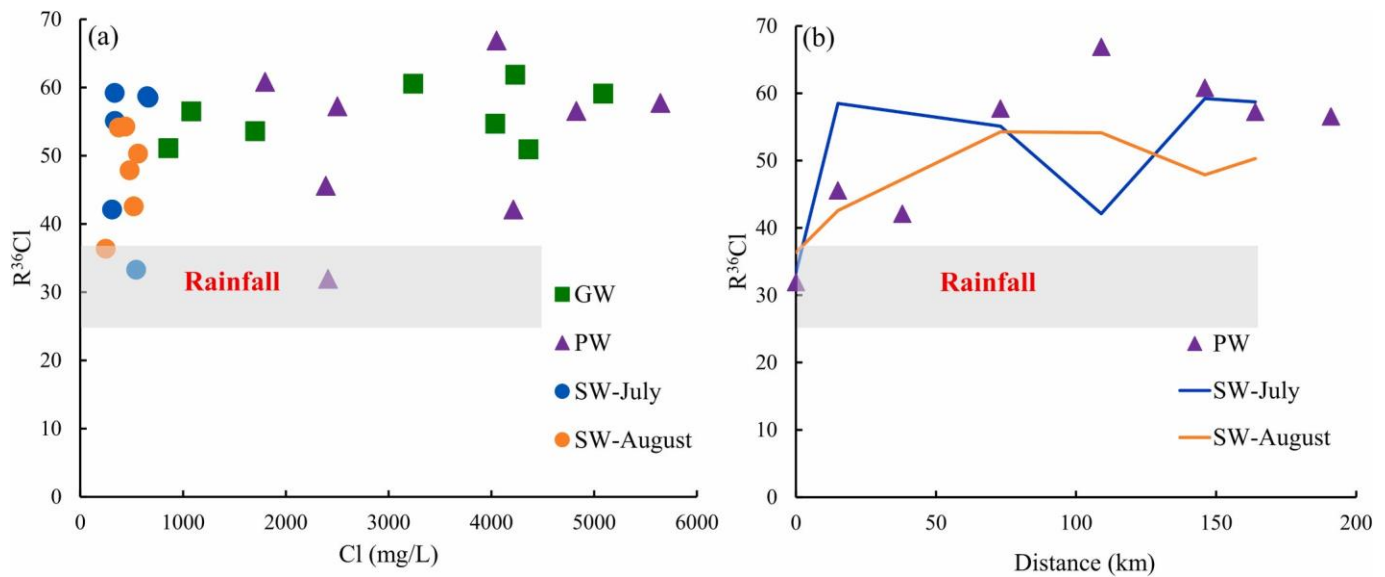


**Fig. 7.**  $R^{36}\text{Cl}$  vs. Cl concentrations (7a) of groundwater (GW), pool water (PW), and stream water (SW) in July and August from the upper Avoca River.  $R^{36}\text{Cl}$  vs. distance (7b) in PW and SW. Shaded areas represent the range of  $R^{36}\text{Cl}$  values in modern rainfall (Howcroft et al., 2019). Data from Tables 1 and 2.

from sporadic rainfall) (Cook et al., 2018). The high  $^3\text{H}$  activities (1.64 to 5.11 TU) recorded in the pool water, however, suggests limited contributions of old regional groundwater (Fig. 6a) indicating much of the water is from younger near-river sources. This conclusion is consistent with the observation that major ion and stable isotope geochemistry of the pool water overlapped with that of the stream water but was different to the groundwater (Figs. 4, 5). The locally high  $^3\text{H}$  activities (up to 5.11 TU) that were recorded at localities downstream of Logan Reserve (Fig. 1) may reflect the input of water derived from late winter and spring rainfall in southeast Australia that has high  $^3\text{H}$  activities due to moisture exchange from the stratosphere-to-the troposphere (Tadros et al., 2014).

Higher  $^3\text{H}$  activities of stream water than those of groundwater (Fig. 6a) and a difference between the stable isotope and major ion geochemistry (Figs. 4, 5) also imply that the river is mainly fed by young water when it is flowing. This is consistent with the observation that the Cl concentrations in the upper Avoca River fluctuate, especially in the middle and lower reaches (Fig. 3b). These fluctuations suggest that the upper Avoca River receives substantial water from low-salinity young near-river sources such as bank storage and return flow, soil water, and/or interflow rather than saline regional groundwater, which would be expected to produce Cl concentrations that increased downstream (Yu et al., 2013; Ortega et al., 2015). Similar behaviour has been documented elsewhere in southeast Australian rivers (e.g., Yu et al., 2013; Zhou and Cartwright, 2021; Barua et al., 2022). Lower  $^3\text{H}$  activities of stream water during the high-flow period in July compared to intermediate flow conditions in August (Table 2) may reflect increased input of regional groundwater or older water from elsewhere in the catchment (e.g., from the soil or the regolith) that was flushed into the river by early rainfall. Input of older water at the onset of flow event has been reported in other Australian catchments and elsewhere (Uhlenbrook et al., 2002; Kirchner, 2003; Unland et al., 2015; Cartwright and Morgenstern, 2016; Tweed et al., 2016; Barua et al., 2022).

## 5.2. Locations of baseflow discharge

Baseflow represents regional groundwater and other younger water sources including water from the riparian zone, bank storage and return flows, soil water, and interflow (McCallum et al., 2010; Cartwright et al., 2014; Cook et al., 2018; Zhou and Cartwright, 2021). Given that the upper Avoca River is probably fed mainly by near-river sources and the  $^{222}\text{Rn}$  activities of these is not known, it is difficult to calculate baseflow fluxes using  $^{222}\text{Rn}$ . Nevertheless,  $^{222}\text{Rn}$  may be used qualitatively to identify the reaches with high relatively baseflow inputs (e.g., Ortega et al., 2015). The  $^{222}\text{Rn}$  activities are highest in the upper parts of the catchment (Fig. 3a). This region contains a number of granites and their weathered products (Fig. 1) that commonly produce high  $^{222}\text{Rn}$  in groundwater. The lower  $^{222}\text{Rn}$  activities downstream (Fig. 3a) likely reflect lower baseflow inputs and/or decreasing  $^{222}\text{Rn}$  activities in the baseflow. While it is difficult to distinguish between these two possibilities, high  $^{222}\text{Rn}$  groundwater exists throughout the catchment (Table S2) and hydraulic gradients, which drive baseflow, are higher in the upper regions of the catchment.

The higher  $^{222}\text{Rn}$  activities in August in the upper Avoca River compared with July imply higher baseflow inputs relative to streamflow (Fig. 3a). This is likely to be a result of the regional water table rising after multiple rainfall events (Fig. 2a), which promotes increased baseflow discharge by hydraulic loading (Voltz et al., 2013). The higher  $^{222}\text{Rn}$  activities (up to 2920 Bq/m<sup>3</sup>) in the headwaters between 0 and 31 km (Fig. 3a) may be due to high relative baseflow inputs caused by the steep topography and consequently high hydraulic gradient in this region. This is consistent with the increase in Cl concentrations in the headwaters (Fig. 3b). The  $^{222}\text{Rn}$  activities in the middle and lower reaches of the river of <1000 Bq/m<sup>3</sup> suggest lower baseflow inputs probably as a result of decreased hydraulic gradients in flat alluvial floodplains.

## 5.3. $R^{36}\text{Cl}$ as a tracer of the solutes

Based on  $^{14}\text{C}$  and  $^3\text{H}$  activities (discussed below), the regional groundwater in the upper Avoca River had MRTs of up to 12,900 years. This timescale is too short for significant decay of  $^{36}\text{Cl}$ , and the  $R^{36}\text{Cl}$  values will largely reflect those when the groundwater was recharged. The modest Cl/Br ratios preclude the Cl in either surface water or groundwater being derived from sources such as halite dissolution on the floodplain, while the stable isotope ratios (Fig. 5) indicate that there is no connate water in the aquifers. The  $R^{36}\text{Cl}$  values of groundwater overlapped with the stream and pool water and were higher than those of modern rainfall in the region (Fig. 6a). High  $R^{36}\text{Cl}$  values were produced during the bomb pulse period; however, the low  $^3\text{H}$  activities and the relatively uniform  $R^{36}\text{Cl}$  values in groundwater that has a range of  $^{14}\text{C}$  activities (Table 1) imply that there is little bomb pulse recharge in the groundwater.  $R^{36}\text{Cl}$  values in Australian rainfall increase



inland due to variations of Cl deposition rates (Keywood et al., 1998; Howcroft et al., 2019) and the high  $R^{36}\text{Cl}$  values are probably due to the groundwater being recharged during the Holocene when sea levels were lower, and the area had a more continental climate. Due to the possible retention of Cl in the catchment by plant uptake or the binding to organic matter in soils (e.g., Howcroft et al., 2019), the Cl residence times may be longer than groundwater residence times, which would allow the preservation of Holocene  $R^{36}\text{Cl}$  values. An increase of  $R^{36}\text{Cl}$  downstream from the headwaters (Fig. 7b) may reflect groundwater entering the river.

Although regional groundwater is not generally well connected to intermittent streams (e.g., Larsen and Woelfle-Erskine, 2018; Zhou et al., 2022), there will still be some localities (e.g., areas that have steep topography with high hydraulic gradients) where some groundwater inflows occur. Because of the high salinity of the groundwater (Table S2), the fluxes of groundwater required to change the  $R^{36}\text{Cl}$  values of the river are probably small.

#### 5.4.1. Mean transit times of stream water

Mixing of rainfall and water stored within the catchment in the pools of the upper Avoca River in the dry seasons means that single lumped parameter models (LPMs) cannot be used to calculate MTTs. While it is possible to use multiple LPMs, there is insufficient data to accurately constrain mixing proportions and the  $^3\text{H}$  activity of the end-members.

As with other studies (Morgenstern et al., 2010; Cartwright and Morgenstern, 2015; Cartwright et al., 2018), MTT estimates for when the river was flowing assume that river is maintained by a single store of water with variable age. This conceptualisation is consistent with the conclusion that the stream water in the upper Avoca River is mostly fed by young water from near-river stores with little input from regional groundwater.

The MTTs in the upper Avoca River when it was flowing varied from 1.4 to 7.0 years (Table 2). MTTs were generally higher in July (4.0 to 7.0 years) and were 1.4 to 4.8 years in August (Table 2). There are several uncertainties in the MTT calculations (e.g., as discussed in detail by Morgenstern et al., 2010; Cartwright and Morgenstern, 2016; Zhou et al., 2022). The different LPMs result in different estimated MTTs. For the upper Avoca River, the highest MTTs (1.5 to 7.0 years) are from the EMM and the lowest (1.4 to 5.5 years) are from the DM with  $D_p$  0.05. This is a relative uncertainty of 17 %. Varying the average annual  $^3\text{H}$  activities of modern rainfall between 2.8 and 3.2 TU produced uncertainties in MTTs of – 33 % to 21 %. A similar relative uncertainty ( $\pm 10$  %) in the  $^3\text{H}$  input function translated to a – 39 % to 46 % uncertainty in the MTTs for these samples.

Aggregation, which refers to the mixing of various water sources with different MTTs, may impact MTT calculations (Suckow, 2014; Kirchner, 2016; Stewart et al., 2017). The effects of aggregation will be most significant when binary mixing between waters with very different MTTs occurs. The calculated MTTs made using  $^3\text{H}$  are less affected if mixing between several water stores occurs because that scenario is comparable to what is modelled using LPMs (Cartwright and Morgenstern, 2016). Aggregation also has less impact if those stores have a relatively small range of MTTs (which is the case in the upper Avoca River).

Despite these uncertainties, the relatively high  $^3\text{H}$  activities imply that upper Avoca River is mostly sustained by relatively young water even when streamflow ceases during the summer. The volume (V) of the reservoir contributing to the river is related to the MTT and streamflow (Q) by  $V = \text{MTT} \times Q$  (Małoszewski and Zuber, 1982) and the short MTTs are consistent with the input of water from relatively small river water stores.

#### 5.4.2. Mean residence times of regional groundwater

Mean residence times of groundwater were estimated using the EPM model (EPM ratio = 0.33; Table 2), which can be employed for groundwater. When the bores sample the deeper, longer flow channels but not the short, near-surface flow paths (Małoszewski and Zuber, 1982). MRTs were calculated using  $^3\text{H}$  activities when these were  $> 0.1$  TU (i.e., significantly above the lower detection limit) and  $^{14}\text{C}$  activities for the rest of the samples. The estimated MRTs of groundwater were between 151 and 12,900 years (Table 1). There is no systematic increase of MRTs with depth or distance from the Avoca River.

Similar uncertainties to those discussed above apply to the MRT estimates and the unknown degree of calcite dissolution adds an additional uncertainty. However, the groundwater is demonstrably several hundreds to thousands of years old. As discussed earlier, the variation in  $^{14}\text{C}$  and  $^3\text{H}$  activities (Fig. 5b) implies that there is limited mixing between regional groundwater and younger recently-recharged water even close to the Avoca River. Only sample 8003933 (site J: Fig. 1) at 60 m depth and 200 m from the river shows mixing between young and old water components. This could be a result of local geology, such as faults or interconnected high permeability layers. However, generally, the Avoca River, which may be locally losing especially at high streamflows, does not recharge the regional groundwater. That conclusion is also consistent with the differences in major ion and stable isotope geochemistry between the river and the groundwater (Figs. 4, 5).

## 6. Conclusions and implications

The combination of major ions, stable isotopes, and radioisotopes allowed the water sources in the intermittent upper Avoca River at different flow conditions, including the dry seasons where the river consists of disconnected pools, to be understood. It illustrates that near-river water stores rather than deeper regional groundwater are important in sustaining streamflow and providing water to the pools. These results are consistent with the conclusions from other intermittent catchments in southeast Australia (Yihdego and Webb, 2013; Dresel et al., 2018; Barua et al., 2022; Zhou et al., 2022) and elsewhere (Costigan et al., 2016; Larsen and Woelfle-Erskine, 2018; Fovet et al., 2021; Shanafield et al., 2021). Despite its importance in understanding the functioning of intermittent catchments, the sources of stream water is not always well understood (e.g., Shanafield et al., 2021; Bourke et al., 2023), and this study thus contributes to a better general understanding of intermittent catchments.

The results have vital implications for the ecosystems that rely on these pools in the summer months. Because the water sources in this catchment are largely derived from the shallow near-river aquifers, maintaining the health of these aquifers and near-river corridor is important in protecting intermittent streams and their ecosystems. Being fed by smaller near-river reservoirs results in these intermittent streams being more vulnerable to short-term climate variations and changes in landuse than comparable perennial streams connected to larger water stores. The conclusion that the intermittent streams have a poor connection to deeper regional groundwater imply that near-river aquifers may act as buffer zones that reduces the rate of contaminated regional groundwater entering the river. Additionally, the effects of regional groundwater pumping on streamflow could also be less.

Intermittent streams may become more prevalent globally in the future due to climate change and extraction of near-river groundwater (Messenger et al., 2021). Catchment intermittency increased in southeast Australia during the Millennium Drought (1996–2010) and the streamflow in many catchments has still not recovered to pre-drought levels (e.g., Peterson et al., 2021). In contrast to intermittent streams, perennial catchments in southeast Australia are sustained by older, larger volume catchment water stores, especially at low streamflows (e.g., Cartwright et al., 2020). Hence, one important consequence of increased intermittency is the possible switch from regional groundwater being an important source of stream water at low flows to streams being sustained mainly by near-river water stores.

This study also illustrates the use of multiple tracers in detecting locations of baseflow discharge and identifying the input of water from stores with different residence times. The conclusion that near-river water sources are important implies that it is difficult to use regional groundwater compositions as end-members to quantify baseflow inputs via  $^{222}\text{Rn}$  and Cl mass balance. The utilization of  $^{36}\text{Cl}$  as a tracer of small influxes of regional groundwater rather than as a residence time indicator represents a potentially important use of this tracer in river catchments. However, to achieve this a more comprehensive understanding of how  $\text{R}^{36}\text{Cl}$  values have varied over time is needed as well as good characterisation of  $\text{R}^{36}\text{Cl}$  values in the various stores of water within catchments. In addition, the study emphasises the use of  $^3\text{H}$  in directly discriminating between young and old water sources. The determination of transit times in perennial streams is relatively commonplace, but studies in intermittent streams are less common and this technique is invaluable in providing direct evidence of water sources. Currently, due to the lower activities of bomb-pulse  $^3\text{H}$ , this is simpler in southern hemisphere catchments (Morgenstern et al., 2010). However, with the bomb-pulse tritium activities declining in the northern hemisphere, this will be more generally applicable.

#### CRediT authorship contribution statement

**Zibo Zhou:** Conceptualization, Investigation, Data curation, Methodology, Writing – original draft, Writing – review & editing. **Ian Cartwright:** Methodology, Resources, Investigation, Writing – review & editing. **Uwe Morgenstern:** Resources, Writing – review & editing. **L. Keith Fifield:** Resources, Writing – review & editing.

#### Declaration of competing interest

The authors declare that they have no known competing financial interests or personal relationships that could have appeared to influence the work reported in this paper.

#### Data availability

Data will be made available on request.

#### Acknowledgements

This work was supported by ARC Special Research Initiative 0800001 and Monash University. Dr. Massimo Raveggi and Rachelle Pierson are thanked for help with the analyses at Monash University. The Heavy Ion Accelerator Facility (HIAF) at ANU is supported by the National Collaborative Research Infrastructure Strategy (NCRIS) of the Australian Government. Ture Carlson is thanked for assisting the sampling. We thank two anonymous referees and the editor for helpful comments that clarified this study.

#### Appendix A. Supplementary data

Supplementary data to this article can be found online at <https://doi.org/10.1016/j.scitotenv.2023.167998>. **References**

- Barua, S., Cartwright, I., Dresel, P.E., Morgenstern, U., McDonnell, J.J., Daly, E., 2022. Sources and mean transit times of intermittent streamflow in semi-arid headwater catchments. *J. Hydrol.* 604, 127208 <https://doi.org/10.1016/j.jhydrol.2021.127208>.
- Battle-Aguilar, J., Harrington, G.A., Leblanc, M., Welch, C., Cook, P.G., 2014. Chemistry of groundwater discharge inferred from longitudinal river sampling. *Water Resour. Res.* 50, 1550–1568. <https://doi.org/10.1002/2013WR013591>.
- Bentley, H.W., Phillips, F.M., Davis, S.N., Gifford, S., Elmore, D., Tubbs, L.E., Gove, H.E., 1982. Thermonuclear  $^{36}\text{Cl}$  pulse in natural water. *Nature* 300, 737–740. <https://doi.org/10.1038/300737a0>.
- Blavoux, B., Lachassagne, P., Henriot, A., Ladouche, B., Marc, V., Beley, J.J., Olive, P., 2013. A fifty-year chronicle of tritium data for characterising the functioning of the Evian and Thonon (France) glacial aquifers. *J. Hydrol.* 494, 116–133. <https://doi.org/10.1016/j.jhydrol.2013.04.029>.
- Bogan, M.T., Leidy, R.A., Neuhaus, L., Hernandez, C.J., Carlson, S.M., 2019. Biodiversity value of remnant pools in an intermittent stream during the great California drought. *Aquat. Conserv. Mar. Freshwat. Ecosyst.* 29, 976–989. <https://doi.org/10.1002/aqc.3109>.
- Bourke, S.A., Shanfield, M., Hedley, P., Chapman, S., Dogramaci, S., 2023. A hydrological framework for persistent pools along non-perennial rivers. *Hydrol. Earth Syst. Sci.* 27, 809–836. <https://doi.org/10.5194/hess-27-809-2023>.
- Brunner, P., Cook, P.G., Simmons, C.T., 2011. Disconnected surface water and groundwater: from theory to practice. *Groundwater* 49, 460–467. <https://doi.org/10.1111/j.1745-6584.2010.00752.x>.
- Bureau of Meteorology, 2022. Australian landscape water balance: Commonwealth of Australia. available at: <http://www.bom.gov.au/water/landscape/>. last access: 20 July 2022.
- Burnett, W.C., Dulaiova, H., 2006. Radon as a tracer of submarine groundwater discharge into a boat basin in Donnalucata, Sicily. *Cont. Shelf Res.* 26, 862–873. <https://doi.org/10.1016/j.csr.2005.12.003>.
- Burnett, W.C., Peterson, R.N., Santos, I.R., Hicks, R.W., 2010. Use of automated radon measurements for rapid assessment of groundwater flow into Florida streams. *J. Hydrol.* 380, 298–304. <https://doi.org/10.1016/j.jhydrol.2009.11.005>.
- Cartwright, I., 2022. Implications of variations in stream specific conductivity for estimating baseflow using chemical mass balance and calibrated hydrograph techniques. *Hydrol. Earth Syst. Sci.* 26, 183–195. <https://doi.org/10.5194/hess-26-183-2022>.
- Cartwright, I., Gilfedder, B., 2015. Mapping and quantifying groundwater inflows to Deep Creek (Maribyrnong catchment, SE Australia) using  $^{222}\text{Rn}$ , implications for protecting groundwater-dependant ecosystems. *Appl. Geochem.* 52, 118–129. <https://doi.org/10.1016/j.apgeochem.2014.11.020>.
- Cartwright, I., Irvine, D., 2020. The spatial extent and timescales of bank infiltration and return flows in an upland river system: implications for water quality and volumes. *Sci. Total Environ.* 140748 <https://doi.org/10.1016/j.scitotenv.2020.140748>.
- Cartwright, I., Morgenstern, U., 2015. Transit times from rainfall to baseflow in headwater catchments estimated using tritium: the Ovens River, Australia. *Hydrol. Earth Syst. Sci.* 19, 3771–3785. <https://doi.org/10.5194/hess-19-3771-2015>.
- Cartwright, I., Morgenstern, U., 2016. Contrasting transit times of water from peatlands and eucalypt forests in the Australian Alps determined by tritium: implications for vulnerability and the source of water in upland catchments. *Hydrol. Earth Syst. Sci.* 20, 4757–4773. <https://doi.org/10.5194/hess-20-4757-2016>.
- Cartwright, I., Gilfedder, B., Hofmann, H., 2013. Chloride imbalance in a catchment undergoing hydrological change: upper Barwon River, Southeast Australia. *Appl. Geochem.* 31, 187–198. <https://doi.org/10.1016/j.apgeochem.2013.01.003>.
- Cartwright, I., Gilfedder, B., Hofmann, H., 2014. Contrasts between estimates of baseflow help discern multiple sources of water contributing to rivers. *Hydrol. Earth Syst. Sci.* 18, 15–30. <https://doi.org/10.5194/hess-18-15-2014>.
- Cartwright, I., Hofmann, H., Currell, M.J., Fifield, L.K., 2017. Decoupling of solutes and water in regional groundwater systems: the Murray Basin, Australia. *Chem. Geol.* 466, 466–478. <https://doi.org/10.1016/j.chemgeo.2017.06.035>.



- Cartwright, I., Atkinson, A.P., Gilfedder, B.S., Hofmann, H., Cendon, D.I., ' Morgenstern, U., 2018. Using geochemistry to understand water sources and transit times in headwater streams of a temperate rainforest. *Appl. Geochem.* 99, 1–12. <https://doi.org/10.1016/j.apgeochem.2018.10.018>.
- Cartwright, I., Werner, A.D., Woods, J.A., 2019. Using geochemistry to discern the patterns and timescales of groundwater recharge and mixing on floodplains in semi- arid regions. *J. Hydrol.* 570, 612–622. <https://doi.org/10.1016/j.jhydrol.2019.01.023>.
- Cartwright, I., Morgenstern, U., Howcroft, W., Hofmann, H., Armit, R., Stewart, M., Irvine, D., 2020. The variation and controls of mean transit times in Australian headwater catchments. *Hydrol. Process.* 34, 4034–4048. <https://doi.org/10.1002/hyp.13862>.
- Cecil, L.D., Green, J.R., 2000. Radon-222. In: *Environmental Tracers in Subsurface Hydrology*. Springer, Boston, MA, pp. 175–194, 2000. [https://doi.org/10.1007/978-1-4615-4557-6\\_6](https://doi.org/10.1007/978-1-4615-4557-6_6).
- Chappell, J.M., 2009. Sea level change, quaternary. In: Gornitz, V. (Ed.), *Encyclopedia of Paleoclimatology and Ancient Environments*. Encyclopedia of Earth Sciences Series. Springer, Dordrecht. [https://doi.org/10.1007/978-1-4020-4411-3\\_208](https://doi.org/10.1007/978-1-4020-4411-3_208).
- Clark, I.D., 2015. *Groundwater Geochemistry and Isotopes*. CRC Press Boca Raton, FL, USA.
- Clark, I.D., Fritz, P., 1997. *Environmental Isotopes in Hydrogeology*. Lewis, New York, p. 328.
- Cook, P.G., 2013. Estimating groundwater discharge to rivers from river chemistry surveys. *Hydrol. Process.* 27, 3694–3707. <https://doi.org/10.1002/hyp.9493>.
- Cook, P.G., Rodellas, V., Stieglitz, T.C., 2018. Quantifying surface water, Porewater, and groundwater interactions using tracers: tracer fluxes, water fluxes, and end-member concentrations. *Water Resour. Res.* 54, 2452–2465. <https://doi.org/10.1002/2017WR021780>.
- Coplen, T.B., 1988. Normalization of oxygen and hydrogen isotope data. *Chem. Geol.* 72, 293–297. [https://doi.org/10.1016/0168-9622\(88\)90042-5](https://doi.org/10.1016/0168-9622(88)90042-5).
- Costigan, K.H., Jaeger, K.L., Goss, C.W., Fritz, K.M., Goebel, P.C., 2016. Understanding controls on flow permanence in intermittent rivers to aid ecological research: integrating meteorology, geology and land cover. *Ecohydrology* 9, 1141–1153. <https://doi.org/10.1002/eco.1712>.
- Datry, T., Larned, S.T., Tockner, K., 2014. Intermittent rivers: a challenge for freshwater ecology. *BioScience* 64 (3), 229–235. <https://doi.org/10.1093/biosci/bit027>.
- Davie, R.F., Calf, G.E., Bird, J.R., Topham, S., Kellett, J.R., Evans, W.R., Ophel, T.R., 1989. Chlorine-36 measurements in the Murray Basin; preliminary results from the Victorian and south Australian Mallee region. *BMR J. Aust. Geol. Geophys.* (Bureau of Mineral Resources, Canberra, Australia) 11, 262–272.
- Davis, S.N., Whittemore, D.O., Fabryka-Martin, J., 1998. Uses of chloride/bromide ratios in studies of potable water. *Ground Water* 36, 338–351. <https://doi.org/10.1111/j.1745-6584.1998.tb01099.x>.
- Department of Environment Land Water and Planning:2022 State Government Victoria, available at: <http://data.water.vic.gov.au/monitoring.htm>, last access: 20 August 2022.
- Department of Jobs, Precincts and Regions, Energy and Earth Resources 2022: State Government Victoria, available at: <http://www.energyandresources.vic.gov.au/earth-resources/maps-reports-and-data/geovic>, last access: 20 August 2022.
- Dresel, P.E., Dean, J.F., Perveen, F., Webb, J.A., Hekmeijer, P., Adelana, S.M., Daly, E., 2018. Effect of Eucalyptus plantations, geology, and precipitation variability on water resources in upland intermittent catchments. *J. Hydrol.* 564, 723–739. <https://doi.org/10.1016/j.jhydrol.2018.07.019>.
- Duvert, C., Stewart, M.K., Cendon, D.I., Raiber, M., 2016. Time series of tritium, stable ' isotopes and chloride reveal short-term variations in groundwater contribution to a stream. *Hydrol. Earth Syst. Sci.* 20, 257–277. <https://doi.org/10.5194/hess-20-257-2016>.
- Edmunds, W.M., 2009. Geochemistry's vital contribution to solving water resource problems. *Appl. Geochem.* 24, 1058–1073. <https://doi.org/10.1016/j.apgeochem.2009.02.021>.
- Fifield, L.K., Tims, S.G., Stone, J.O., Argento, D.C., De Cesare, M., 2013. Ultra-sensitive measurements of <sup>36</sup>Cl and <sup>236</sup>U at the Australian National University. *Nucl. Instrum. Methods Phys. Res., Sect. B* 294, 126–131. <https://doi.org/10.1016/j.nimb.2012.04.028>.
- Fleckenstein, J.H., Krause, S., Hannah, D.M., Boano, F., 2010. Groundwater-surface water interactions: new methods and models to improve understanding of processes and dynamics. *Adv. Water Resour.* 33, 1291–1295. <https://doi.org/10.1016/j.advwatres.2010.09.011>.
- Fovet, O., Belemtougri, A., Boithias, L., Braud, I., Charlier, J.B., Cottet, M., Datry, T., 2021. Intermittent rivers and ephemeral streams: perspectives for critical zone science and research on socio-ecosystems. *Wiley Interdiscip. Rev. Water* 8, e1523. <https://doi.org/10.1002/wat2.1523>.
- Fowler, K., Peel, M., Saft, M., Peterson, T., Western, A., Band, L., Nathan, R., 2022. Explaining changes in rainfall-runoff relationships during and after Australia's millennium drought: a community perspective. *Hydrol. Earth Syst. Sci.* 26, 6073–6120. <https://doi.org/10.5194/hess-26-6073-2022>.
- Fuchs, E.H., King, J.P., Carroll, K.C., 2019. Quantifying disconnection of groundwater from managed-ephemeral surface water during drought and conjunctive agricultural use. *Water Resour. Res.* 55, 5871–5890. <https://doi.org/10.1029/2019WR02494>.
- Genereux, D.P., Hemond, H.F., 1992. Determination of gas exchange rate constants for a small stream on Walker branch watershed, Tennessee. *Water Resour. Res.* 28, 2365–2374. <https://doi.org/10.1029/92WR01083>.
- Gonfiantini, R., 1986. *Environmental isotopes in lake studies*. In: *Handbook of Environmental Isotope Geochemistry*, 2, pp. 113–168.
- Gutiérrez-Jurado, K.Y., Partington, D., Batelaan, O., Cook, P., Shanafield, M., 2019. What triggers streamflow for intermittent rivers and ephemeral streams in low-gradient catchments in Mediterranean climates. *Water Resour. Res.* 55, 9926–9946. <https://doi.org/10.1029/2019WR025041>.
- Heislors, D., 1993. *Groundwater in the Central Victorian Highlands*. Report No. 87. Department of Conservation and Natural Resources, Water Division, Melbourne.
- Herczeg, A.L., Dogramaci, S.S., Leaney, F.W., 2001. Origin of dissolved salts in a large, semi-arid groundwater system: Murray Basin, Australia. *Mar. Freshw. Res.* 52, 41–52. <https://doi.org/10.1071/MF00040>.
- Hollins, S.E., Hughes, C.E., Crawford, J., Cendon, D.I., Meredith, K.T., 2018. Rainfall ' isotope variations over the Australian continent—implications for hydrology and isoscape applications. *Sci. Total Environ.* 645, 630–645. <https://doi.org/10.1016/j.scitotenv.2018.07.082>.
- Howcroft, W., Cartwright, I., Morgenstern, U., 2018. Mean transit times in headwater catchments: insights from the Otway ranges, Australia. *Hydrol. Earth Syst. Sci.* 22, 635–653. <https://doi.org/10.5194/hess-22-635-2018>.
- Howcroft, W., Cartwright, I., Cendon, D.I., 2019. Residence times of bank storage and ' return flows and the influence on river water chemistry in the upper Barwon River, Australia. *Appl. Geochem.* 101, 31–41. <https://doi.org/10.1016/j.apgeochem.2018.12.026>.
- Hughes, C.E., Crawford, J., 2012. A new precipitation weighted method for determining the meteoric water line for hydrological applications demonstrated using Australian and global GNIP data. *J. Hydrol.* 464, 344–351. <https://doi.org/10.1016/j.jhydrol.2012.07.029>.
- Jurgens, B.C., Bohkle, J.K., Eberts, S.M., 2012. TracerLPM (Version 1): An Excel® Workbook for Interpreting Groundwater Age Distributions from Environmental Tracer Data, United States Geological Survey. Techniques and Methods Report 4-F3., United States Geological Survey, Reston, USA. <https://doi.org/10.3133/tm4F3>, 60 pp.
- Keywood, M.D., Fifield, L.K., Chivas, A.R., Cresswell, R.G., 1998. Fallout of chlorine 36 to the Earth's surface in the southern hemisphere. *J. Geophys. Res.* 103 (D7), 8281–8286. <https://doi.org/10.1029/97JD03125>.
- Kirchner, J.W., 2003. A double paradox in catchment hydrology and geochemistry. *Hydrol. Process.* 17, 871–874. <https://doi.org/10.1002/hyp.5108>.
- Kirchner, J.W., 2016. Aggregation in environmental systems—part 1: seasonal tracer cycles quantify young water fractions, but not mean transit times, in spatially heterogeneous catchments. *Hydrol. Earth Syst. Sci.* 20, 279–297. <https://doi.org/10.5194/hess-20-279-2016>.
- Labotka, D.M., Panno, S.V., Locke, R.A., Freiburg, J.T., 2015. Isotopic and geochemical characterization of fossil brines of the Cambrian Mt. Simon Sandstone and Ironton–Galesville Formation from the Illinois Basin, USA. *Geochim. Cosmochim. Acta* 165, 342–360. <https://doi.org/10.1016/j.gca.2015.06.013>.
- Larsen, L.G., Woelfle-Erskine, C., 2018. Groundwater is key to salmonid persistence and recruitment in intermittent Mediterranean-climate streams. *Water Resour. Res.* 54, 8909–8930. <https://doi.org/10.1029/2018WR023324>.
- Le Gal La Salle, C., Marlin, C., Leduc, C., Taupin, J.D., Massault, M., Favreau, G., 2001. Renewal rate estimation of groundwater based on radioactive tracers (<sup>3</sup>H, <sup>14</sup>C) in an unconfined aquifer in a semi-arid area, Iullemeden Basin. *Niger. J. Hydrol.* 254, 145–156. [https://doi.org/10.1016/S0022-1694\(01\)00491-7](https://doi.org/10.1016/S0022-1694(01)00491-7).
- Lewandowski, J., Meinikmann, K., Krause, S., 2020. Groundwater–surface water interactions: recent advances and interdisciplinary challenges. *Water* 12, 296. <https://doi.org/10.3390/w12010296>.
- Lewis, S.E., Sloss, C.R., Murray-Wallace, C.V., Woodroffe, C.D., Smithers, S.G., 2013. Post-Glacial Sea-level changes around the Australian margin: a review. *Quat. Sci. Rev.* 74, 115–138. <https://doi.org/10.1016/j.quascirev.2012.09.006>.
- Lorimer, M.S., Rowan, J.N., 1982. *A Study of the Land in the Catchment of the Avoca River*. Soil Conservation Authority.

- Maloszewski, P., 2000. Lumped-parameter models as a tool for determining the hydrological parameters of some groundwater systems based on isotope data, in: tracer and modelling in hydrogeology-Proceedings of the TraM'2000 conference, may 2020, Liege, Belgium, IAHS Publ. No. 262, 271–276, ISBN 190150221X.
- Maloszewski, P., Zuber, A., 1982. Determining the turnover time of groundwater systems with the aid of environmental tracers: 1. Models and their applicability. *J. Hydrol.* 57, 207–231. [https://doi.org/10.1016/0022-1694\(82\)90147-0](https://doi.org/10.1016/0022-1694(82)90147-0).
- McCallum, J.L., Cook, P.G., Brunner, P., Berhane, D., 2010. Solute dynamics during bank storage flows and implications for chemical base flow separation. *Water Resour. Res.* 46, W07541. <https://doi.org/10.1029/2009WR008539>.
- McCallum, J.L., Cook, P.G., Berhane, D., Rumpf, C., McMahon, G.A., 2012. Quantifying groundwater flows to streams using differential flow gauging and water chemistry. *J. Hydrol.* 416, 118–132. <https://doi.org/10.1016/j.jhydrol.2011.11.040>.
- McCormac, F.G., Hogg, A.G., Blackwell, P.G., Buck, C.E., Higham, T.F., Reimer, P.J., 2004. SHCal04 southern hemisphere calibration, 0–11.0 cal kyr BP. *Radiocarbon* 46, 1087–1092. <https://doi.org/10.1017/S0033822200033014>.
- McGuire, K.J., McDonnell, J.J., 2006. A review and evaluation of catchment transit time modelling. *J. Hydrol.* 330, 543–563. <https://doi.org/10.1016/j.jhydrol.2006.04.020>.
- Meredith, K.T., Han, L.F., Hollins, S.E., Cendon, D.I., Jacobsen, G.E., Baker, A., 2016. Evolution of chemical and isotopic composition of inorganic carbon in a complex semi-arid zone environment: consequences for groundwater dating using radiocarbon. *Geochim. Cosmochim. Acta* 188, 352–367. <https://doi.org/10.1016/j.gca.2016.06.011>.
- Messenger, M.L., Lehner, B., Cockburn, C., Lamouroux, N., Pella, H., Snelder, T., Detry, T., 2021. Global prevalence of non-perennial rivers and streams. *Nature* 594, 391–397. <https://doi.org/10.1038/s41586-021-03565-5>.
- Miller, M.P., Johnson, H.M., Susong, D.D., Wolock, D.M., 2015. A new approach for continuous estimation of baseflow using discrete water quality data: method description and comparison with baseflow estimates from two existing approaches. *J. Hydrol.* 522, 203–210. <https://doi.org/10.1016/j.jhydrol.2014.12.039>.
- Morgenstern, U., Taylor, C.B., 2009. Ultra low-level tritium measurement using electrolytic enrichment and LSC. *Isot. Environ. Health Stud.* 45, 96–117. <https://doi.org/10.1080/10256010902931194>.
- Morgenstern, U., Stewart, M.K., Stenger, R., 2010. Dating of streamwater using tritium in a post nuclear bomb pulse world: continuous variation of mean transit time with streamflow. *Hydrol. Earth Syst. Sci.* 14, 2289–2301. <https://doi.org/10.5194/hess-14-2289-2010>.
- Morgenstern, U., Daughney, C.J., Leonard, G., Gordon, D., Donath, F.M., Reeves, R., 2015. Using groundwater age and hydrochemistry to understand sources and dynamics of nutrient contamination through the catchment into Lake Rotorua, New Zealand. *Hydrol. Earth Syst. Sci.* 19, 803–822. <https://doi.org/10.5194/hess-19-803-2015>.
- Niswonger, R.G., Prudic, D.E., Fogg, G.E., Stonestrom, D.A., Buckland, E.M., 2008. Method for estimating spatially variable seepage loss and hydraulic conductivity in intermittent and ephemeral streams. *Water Resour. Res.* 44 <https://doi.org/10.1029/2007WR006626>.
- North Central Catchment Management Authority, 2007. Avoca Catchment Local Management Plan.
- Ortega, L., Manzano, M., Custodio, E., Hornero, J., Rodríguez-Arevalo, J., 2015. Using  $^{222}\text{Rn}$  to identify and quantify groundwater inflows to the Mundo River (SE Spain). *Chem. Geol.* 395, 67–79. <https://doi.org/10.1016/j.chemgeo.2014.12.002>.
- Peters, N.E., Burns, D.A., Aulenbach, B.T., 2014. Evaluation of high-frequency mean streamwater transit-time estimates using groundwater age and dissolved silica concentrations in a small forested watershed. *Aquat. Geochem.* 20, 183–202. <https://doi.org/10.1007/s10498-013-9207-6>.
- Peterson, T.J., Saft, M., Peel, M.C., John, A., 2021. Watersheds may not recover from drought. *Science* 372, 745–749. <https://doi.org/10.1126/science.abd5085>.
- Phillips, F.M., 2000. Chloride-36. In: Cook, P., Herczeg, A. (Eds.), *Environmental Tracers in Subsurface Hydrology*. Kluwer Academic Publishers, Boston, pp. 299–348.
- Reimer, P.J., Bard, E., Bayliss, A., Beck, J.W., Blackwell, P.G., Ramsey, C.B., Van Der Plicht, J., 2013. IntCal13 and Marine13 radiocarbon age calibration curves 0–50,000 years cal BP. *Radiocarbon* 55, 1869–1887. [https://doi.org/10.2458/azu\\_js\\_rc.55.16947](https://doi.org/10.2458/azu_js_rc.55.16947).
- Rhodes, K.A., Proffitt, T., Rowley, T., Knappett, P.S., Montiel, D., Dimova, N., Miller, G. R., 2017. The importance of bank storage in supplying baseflow to rivers flowing through compartmentalized, alluvial aquifers. *Water Resour. Res.* 53, 10539–10557. <https://doi.org/10.1002/2017WR021619>.
- Richardson, C.M., Zimmer, M.A., Fackrell, J.K., Paytan, A., 2020. Geologic controls on source water drive baseflow generation and carbon geochemistry: evidence of nonstationary baseflow sources across multiple subwatersheds. *Water Resour. Res.* 56 <https://doi.org/10.1029/2019WR026577> e2019WR026577.
- Shanfield, M., Bourke, S.A., Zimmer, M.A., Costigan, K.H., 2021. An overview of the hydrology of non-perennial rivers and streams. *Wiley Interdiscip. Rev. Water* 8, e1504. <https://doi.org/10.1002/wat2.1504>.
- Smith, N., 1995. Recent hydrological changes in the Avoca River catchment, Victoria. *Aust. Geogr. Stud.* 33, 6–18. <https://doi.org/10.1111/j.1467-8470.1995.tb00681.x>.
- Sophocleous, M., 2002. Interactions between groundwater and surface water: the state of the science. *Hydrogeol. J.*, 10, 52–67. <https://doi.org/10.1007/s1007/s10040-014-1215-0>.
- Stelzer, R.S., Thad Scott, J., Bartsch, L.A., Parr, T.B., 2014. Particulate organic matter quality influences nitrate retention and denitrification in stream sediments: evidence from a carbon burial experiment. *Biogeochemistry* 119, 387–402. <https://doi.org/10.1007/s10533-014-9975-0>.
- Stewart, M.K., Thomas, J.T., Norris, M., Trompeter, V., 2004. Paleogroundwater in the Moutere gravel aquifers near Nelson, New Zealand. *Radiocarbon* 46, 517–529. <https://doi.org/10.1017/S0033822200035578>.
- Stewart, M.K., Morgenstern, U., Gusyev, M.A., Maloszewski, P., 2017. Aggregation effects on tritium-based mean transit times and young water fractions in spatially heterogeneous catchments and groundwater systems. *Hydrol. Earth Syst. Sci.* 21, 4615–4627. <https://doi.org/10.5194/hess-21-4615-2017>.
- Stubbington, R., England, J., Wood, P.J., Sefton, C.E., 2017. Temporary streams in temperate zones: recognizing, monitoring and restoring transitional aquatic-terrestrial ecosystems. *Wiley Interdiscip. Rev. Water* 4, e1223. <https://doi.org/10.1002/wat2.1223>.
- Suckow, A., 2014. The age of groundwater—definitions, models and why we do not need this term. *Appl. Geochem.* 50, 222–230. <https://doi.org/10.1016/j.apgeochem.2014.04.016>.
- Tadros, C.V., Hughes, C.E., Crawford, J., Hollins, S.E., Chisari, R., 2014. Tritium in Australian precipitation: a 50-year record. *J. Hydrol.* 513, 262–273. <https://doi.org/10.1016/j.jhydrol.2014.03.031>.
- Tetzlaff, D., Soulsby, C., 2008. Sources of baseflow in larger catchments—using tracers to develop a holistic understanding of runoff generation. *J. Hydrol.* 359, 287–302. <https://doi.org/10.1016/j.jhydrol.2008.07.008>.
- Tweed, S., Munksgaard, N., Marc, V., Rockett, N., Bass, A., Forsythe, A.J., Bird, M.I., Leblanc, M., 2016. Continuous monitoring of stream  $\delta^{18}\text{O}$  and  $\delta^2\text{H}$  and stormflow hydrograph separation using laser spectrometry in an agricultural catchment. *Hydrol. Process.* 30, 648–660. <https://doi.org/10.1002/hyp.10689>.
- Uhlenbrook, S., Frey, M., Leibundgut, C., Maloszewski, P., 2002. Hydrograph separations in a mesoscale mountainous basin at event and seasonal timescales. *Water Resour. Res.* 38, 311–3114. <https://doi.org/10.1029/2001WR000938>.
- Unland, N.P., Cartwright, I., Daly, E., Gilfedder, B.S., Atkinson, A.P., 2015. Dynamic river-groundwater exchange in the presence of a saline, semi-confined aquifer. *Hydrol. Process.* 29, 4817–4829. <https://doi.org/10.1002/hyp.10525>.
- Voltz, T., Gooseff, M., Ward, A.S., Singha, K., Fitzgerald, M., Wagener, T., 2013. Riparian hydraulic gradient and stream-groundwater exchange dynamics in steep headwater valleys. *J. Geophys. Res.* Earth 118, 953–969. <https://doi.org/10.1002/jgrf.20074>.
- Yihdego, Y., Webb, J., 2013. An empirical water budget model as a tool to identify the impact of land-use change in stream flow in southeastern Australia. *Water Resour. Manag.* 27, 4941–4958. <https://doi.org/10.1007/s11269-013-0449-2>.
- Yu, M.C.L., Cartwright, I., Braden, J.L., De Bree, S.T., 2013. Examining the spatial and temporal variation of groundwater inflows to a valley-to-floodplain river using  $^{222}\text{Rn}$ , geochemistry and river discharge: the Ovens River, Southeast Australia. *Hydrol. Earth Syst. Sci.* 17, 4907–4924. <https://doi.org/10.5194/hess-17-4907-2013>.
- Zhang, R., Li, Q., Chow, T.L., Li, S., Danieleescu, S., 2013. Baseflow separation in a small watershed in New Brunswick, Canada, using a recursive digital filter calibrated with the conductivity mass balance method. *Hydrol. Process.* 27, 2659–2665. <https://doi.org/10.1002/hyp.9417>.
- Zhou, Z., Cartwright, I., 2021. Using geochemistry to identify and quantify the sources, distribution, and fluxes of baseflow to an intermittent river impacted by climate change: the upper Wimmera River, Southeast Australia. *Sci. Total Environ.* 801, 149725 <https://doi.org/10.1016/j.scitotenv.2021.149725>.
- Zhou, Z., Cartwright, I., Morgenstern, U., 2022. Sources and mean transit times of stream water in an intermittent river system: the upper Wimmera River, Southeast Australia. *Hydrol. Earth Syst. Sci.* 26, 4497–4513. <https://doi.org/10.5194/hess-26-4497-2022>.
- Zuber, A., Maloszewski, P., 2001. Lumped parameter models. In: Mook, W.G., Yurtsever, Y. (Eds.), chap. 2, vol 6: *Modelling in Environmental Isotopes in the Hydrological Cycle: Principles and Applications*, Technical Documents in Hydrology, 39. UNESCO, Paris, France, pp. 5–35.